Reaction Chemistry & Engineering

Linking fundamental chemistry and engineering to create scalable, efficient processes

Accepted Manuscript

This article can be cited before page numbers have been issued, to do this please use: Y. Zhu, Q. Chen, L. Shao, Y. Jia and X. Zhang, *React. Chem. Eng.*, 2019, DOI: 10.1039/C9RE00217K.




ROYAL SOCIETY OF CHEMISTRY

rsc.li/reaction-engineering

View Article Online
DOI: 10.1039/C9RE00217K



# Microfluidic immobilized enzyme reactors for continuous biocatalysis

**Yujiao Zhu [a, b, c], Qingming Chen [a, b], Liyang Shao[d], Yanwei Jia [c, e, f] and Xuming Zhang [a, b, *]**

## Abstract

Biocatalysis has attracted significant attention owing to their environmental-friendly nature, high efficiency and remarkable selectivity during reactions. However, enzymes, one powerful catalyst used in biocatalysis, suffer from low stability for long time operation in solution and gradual decrease of activity in storage. Microfluidic reactors are devices known for small dimension, large surface to volume ratio and well-defined reaction time. Enzymes immobilized in the microfluidic reactors can bring in clear benefits such as fast reaction rate, high storage stability, suppressed autolysis and ease of use. The use of microfluidic immobilized enzyme reactors (μ-IMERs) offers several advantages over traditional technologies in performing biocatalytic reactions, such as low

[a] Department of Applied Physics, The Hong Kong Polytechnic University, Hong Kong, China

[b] The Hong Kong Polytechnic University Shenzhen Research Institute, Shenzhen, China

[c] State Key Laboratory of Analog and Mixed Signal VLSI, Institute of Microelectronics, University of Macau, Macau, China

[d] Department of Electrical and Electronic Engineering, Southern University of Science and Technology, Shenzhen, China

[e] Faculty of Science and Technology, University of Macau, Macau, China

[f] Faculty of Health Sciences, University of Macau, Macau, China

[*] Correspondence: e-mail:apzhang@polyu.edu.hk

View Article Online
DOI: 10.1039/C9RE00217K

energy consumption, rapid heat exchange, fast mass transfer, high efficiency and superior repeatability. In this review, the strategies of employing μ-IMERs for continuous biocatalysis will be investigated by a top-down approach. First, from the macroscopic perspective, the fabrication techniques of the microfluidic reactors are presented in the aspects of the materials, the configurations and the technologies. Then, from the microscopic point of view, several strategies are discussed for the internal structural designs of microfluidic reactors. Moreover, when we move to a nanoscopic level, attention is paid to the choice of enzyme immobilization techniques for the performance enhancement. Finally, the scalability of microfluidics which transfers the biocatalysis from laboratory try to industrial production is investigated. This review is intended to provide a guide to the biocatalysis in microreactors and to expediting the progress of this important research area.

**Keywords:** *in vitro* biocatalysis; microfluidic reactor; enzyme immobilization; multi-enzyme systems; scalability

View Article Online
DOI: 10.1039/C9RE00217K



# 1. Introduction

Biocatalysis is regarded as the most important green research area for sustainable manufacturing in the pharmaceutical and fine chemicals industries due to its low operating costs and high eco-efficiency.[1] Enzyme is one important kind of natural catalysts for biocatalysis which owns many excellent characteristics that artificial catalysts are lack of, such as high efficiency, great selectivity, environment friendly and the ability to catalyze the reaction under mild conditions.[2] The applications of enzyme for green and sustainable chemical synthesis in industry have also infiltrated into our daily life. Despite this, enzyme still need to be improved on some certain aspects prior to being applied to the mass production of industrialized products, such as reusability and activity recovery for economic effects, long-term operation and storage stability, inhibition of certain reaction products, and selectivity to non-native substrates.[3] Moreover, the separation of enzyme from products after the completion of reaction, though costs time and effort, is always an indispensable part of work. Possible contamination of the products should be avoided and the overall operational costs could be reduced.[4] Fortunately, the technique of enzyme immobilization provides an impressive way to overcome these drawbacks. It greatly simplifies the separation and recovery of enzyme. The activity, stability and selectivity of enzyme can also be improved after immobilization.[5] Researchers have devoted lots efforts to studying various enzyme immobilization techniques so far, including physical adsorption, affinity bonding, covalent binding, and encapsulation.[6-9] Nevertheless, inappropriate immobilization would also cause conformational change, block of active sites and diffusion resistance to the enzyme, which in turn results in the activity loss. Considering the structural diversity, complexity and variability of enzymes and their sensitivity to environmental conditions, the selection of immobilization technique should be very careful with specific analysis. The exploration of simple, efficient and widely adaptable enzyme

View Article Online
DOI: 10.1039/C9RE00217K

immobilization methods should also get more attention.

In laboratory research of enzyme immobilization, a higher yield can be obtained if the products are separated from the enzymes in time and the substrates are continuously supplemented.[10] Therefore, the application of enzyme immobilization in continuous microfluidic reactors attracts a lot of interests in industrial production like the synthesis of petrochemicals, active pharmaceutical ingredients or value-added materials.[11-13] Continuous microfluidic system outperforms batch system with many advantages, such as small dimension, low cost and energy consumption, high efficiency, rapid heat exchange and fast mass transfer.[14-16] Specifically, the large surface area to volume (SAV) ratio in microfluidic reactors is advantageous for the enzyme loading. Different microchannel types (e.g., wall-coated type, packed-bed type, and monolithic type) also provide various possibilities for the integration of immobilization carriers into micro space. When the enzyme is immobilized in microfluidic reactors, there is no need to separate the enzyme loaded carriers from the reaction solution, which facilitates recovery and reusability of enzyme, therefore saving the time and labor. Moreover, different catalytic reaction conditions (such as temperature, pH, residence time, and pressure) are easier to control in microfluidic reactors as compared to the operation in batch systems.[17] Higher temperature with low-boiling solvents, higher pressure, more uniform heat/pressure distribution, safer and easier reaction control and less unwanted products can be achieved.[18] Furthermore, the stop of reactions can be easily achieved by pumping the substrate out of the reactors without the need for the addition of acid or base that may affect the detection accuracy or products. Then the microfluidic reactors can be directly incorporated into many instruments for real-time analysis and monitoring. Besides, many natural biocatalytic reactions are cascaded multi-enzymatic reactions.[19] Immobilizing enzymes in the microfluidic reactors make it easy to control their sequential order and relative position, thus

View Article Online
DOI: 10.1039/C9RE00217K



reverting the natural cascaded reactions to a maximum extent. In addition, microfluidic reactors are easily to be scaled up or scaled out once careful design factors are taken into account.[20] In general, these great features of continuous microfluidic immobilized enzyme reactors (μ-IMERs) hold the key for them to be applied in green, sustainable, economical and large-scale industrial production.[21-23]

This review gives a comprehensive discussion on the factors that affect the performance of continuous biocatalysis in the μ-IMERs using a top-down strategy. From the macroscopic point of view, the first thing to consider is the fabrication of microfluidic reactors as well as the materials and the configuration designs. Various materials have been developed in microfluidics, such as silicon, glass, polymers and paper. The characteristics of fabrication materials are of vital importance to the performance of catalytic reactions. Special biocatalysis can also be achieved with careful design of the configuration of the device. From the microscopic point of view, the capacity of inner structures of microreactors for enzyme loading also plays a significant role in the overall biocatalytic efficiency. In addition, the specific substrate diffusion path induced by different types of microreactors should also be taken into account. Moreover, from the nanoscopic point of view, different immobilization techniques, which dominate the performance of enzymes such as their activity, stability and reusability in the nano-environment of biocatalytic reactions, are also thoroughly studied. Finally, the scalability of microfluidics which transfers the biocatalysis in laboratory to that in industry for large amount production is briefly reviewed. We hope the discussion in this review can help understand the main characteristics of the rapidly developing μ-IMERs for continuous biocatalysis and can provide a clear guide to the future research.

View Article Online
DOI: 10.1039/C9RE00217K



# 2. Engineering of microfluidic reactors

## 2.1 Materials for microfluidic reactors

There are many materials that have been used for the fabrication of microfluidic reactors. The basic characteristics are stable and inert.[24] In early days, silicon[25] and glass were mostly used, which directly inherited from the semiconductor industry and the microelectromechanical systems (MEMS).[26] They usually require the surface salinization and the introduction of some functional groups such as carboxyl groups or amino groups for further immobilization.[27] While the high cost and complicated fabrication procedures of them usually limit their applications in microfluidics. Therefore, many polymers with easy fabrication and high compatibility for the biocatalysis have gained significant interest in microfluidics.

As one typical silicon-based organic polymer, polydimethylsiloxane (PDMS) is very popular in the bio-microfluidics application. It is advantageous in excellent biocompatibility, easy fabrication, low cost and optical transparency which is beneficial for the monitor and optical detection of the biocatalytic reaction.[28] The flexible feature also makes PDMS an excellent material to fabricate valves and pumps in microfluidic devices. Nevertheless, some problems of PDMS are not negligible: the swelling in some organic solvents, the change of solution concentration due to the water evaporation and the hydrophobic surface which leads to the non-specific adsorption of biomolecules. Thus, oxygen plasma or surface modification are usually required to make it hydrophilic and to introduce functional groups for enzyme immobilization.

Some other polymer materials, such as polymethylmethacrylate (PMMA)[29-31], polystyrene (PS)[32], polycarbonate (PC)[33], poly (ethylene terephthalate) (PET)[34] and polytetrafluoroethylene (PTFE) [35,36], are also widely used for microfluidics fabrication. Though possessing excellent

View Article Online
DOI: 10.1039/C9RE00217K



chemical, electrical, mechanical, optical and thermal properties,[37-40] they usually also require additional surface modification due to the lack of functional groups on the surfaces. Sometimes stainless steel and ceramic are used for the reactor fabrication if the reaction is operated under high temperature and high pressure.[41] But their high fabrication cost largely restricts their broad applications. Ogończyk *et al*. firstly used PC microchannels for enzyme immobilization in 2012.[33] The PC microfluidic chip was able to immobilize different kinds of enzymes like alkaline phosphatase (ALP) and urease by the physical-chemical method. And the enzymatic microfluidic chips also present attractive operation reproducibility, storage stability and high conversion rates.

Paper is another promising material for microfluidic reactors fabrication. Paper-based microfluidics generally have porous and open channels, which provide larger surface areas for enzyme immobilization as compared to the conventional microfluidics which have only hollow channels. However, the paper-based microfluidics are mainly used for biochemical analysis, medical diagnostics and forensic diagnostics,[42,43] which are not in the scope of this review.

## 2.2 Configuration design of microfluidic reactors

The configuration of microfluidic reactors is varied in different situations. Four representative configuration designs are illustrated in Fig. 1. The single-channel microfluidic chip is the simplest type. It has only one straight channel for the immobilization of enzyme and the transport of substrate (Fig. 1a). The open-tubular or capillaries can also be classified into this category. Nevertheless, the volume of the single-channel microfluidic chip is generally limited for the enzyme loading. The serpentine channel (or curved channel) is accordingly designed by folding up the single channel into the serpentine (curved) shape to increase the effective volume for immobilization (Fig. 1b). The multi-channel microfluidic chip is a more advanced design that multiplies the effective immobilization volume.[44] As shown in Fig.1c, the microchannels are

View Article Online
DOI: 10.1039/C9RE00217K



divided into an array on the input side and a similar unit on the output side. For further volume increase, the planar microfluidic chip is presented by simply enlarging the channel into a planar chamber in the lateral direction (Fig. 1d).

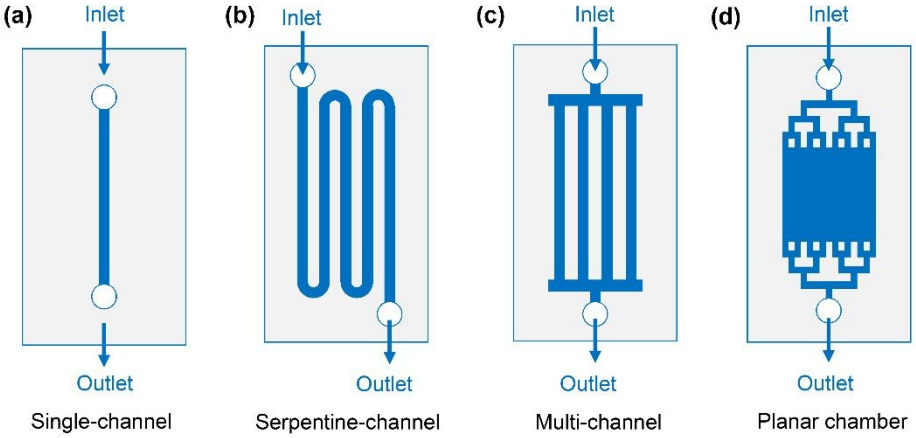


Fig. 1 Representative configuration designs of microfluidic chips.

The configuration of microfluidic reactors should be well designed when applied to continuous biocatalysis. In the bulk system, the substrate solutions react with the enzymes by mixing and diffusion. The reaction performance is unlikely influenced by the container shape. While in microfluidic chip, the substrate solutions are driven by external forces to react with the enzymes immobilized in the chip. If the immobilization amount of enzyme and the residence time of the biocatalysis are fixed, the configuration design would have a great impact on the accessibility of the substrate to the immobilized enzyme and then affects the overall biocatalytic reaction performance.[45] Hoffmann *et al*. designed four HRP-immobilized microreactors with different configurations: full surface, half surface, fine checker-board and coarse checker-board.[46] Fig. 2a shows the product absorbance at the reactor outlet for each pattern. The fine and the coarse checkerboard structures exhibited an increased efficiency with 81% and 56% higher absorbance per active area than the fully modified surface. Different configurations would result in different

View Article Online
DOI: 10.1039/C9RE00217K



velocities across the reactors, therefore influencing the mass transport and mixing of the fluid. Consequently, the accessibility of substrate for the enzyme near the surface is affected, leading to the difference in the reaction performance.

It has also been proved by Nakagawa et al. that channel shape has a great impact on the backpressure which further affects the enzyme activity.[47] Five microreactors with different numbers and lengths of elbow and straight sections were prepared. Protease was immobilized in a freeze-dried poly(vinyl alcohol) (PVA) micro monolith prepared in the microreactors. The proteolytic reaction yields of the five reactors obtained in the same resident time were significantly different due to the changes in the elbow and straight sections, as shown in Fig. 2 c-g. The microreactor with the least number of elbow sections had the highest reaction yield but the smallest pressure drop (Fig. 2h). The pressure drop is related to the resultant fluid resistance, which is determined by the microchannel patterning. Therefore, the accessibility of substrate to the immobilized enzyme via diffusion is largely affected, resulting in the differences in the reaction yields. Then the microreactor with the smallest pressure drop would have the highest enzyme activity.

View Article Online
DOI: 10.1039/C9RE00217K



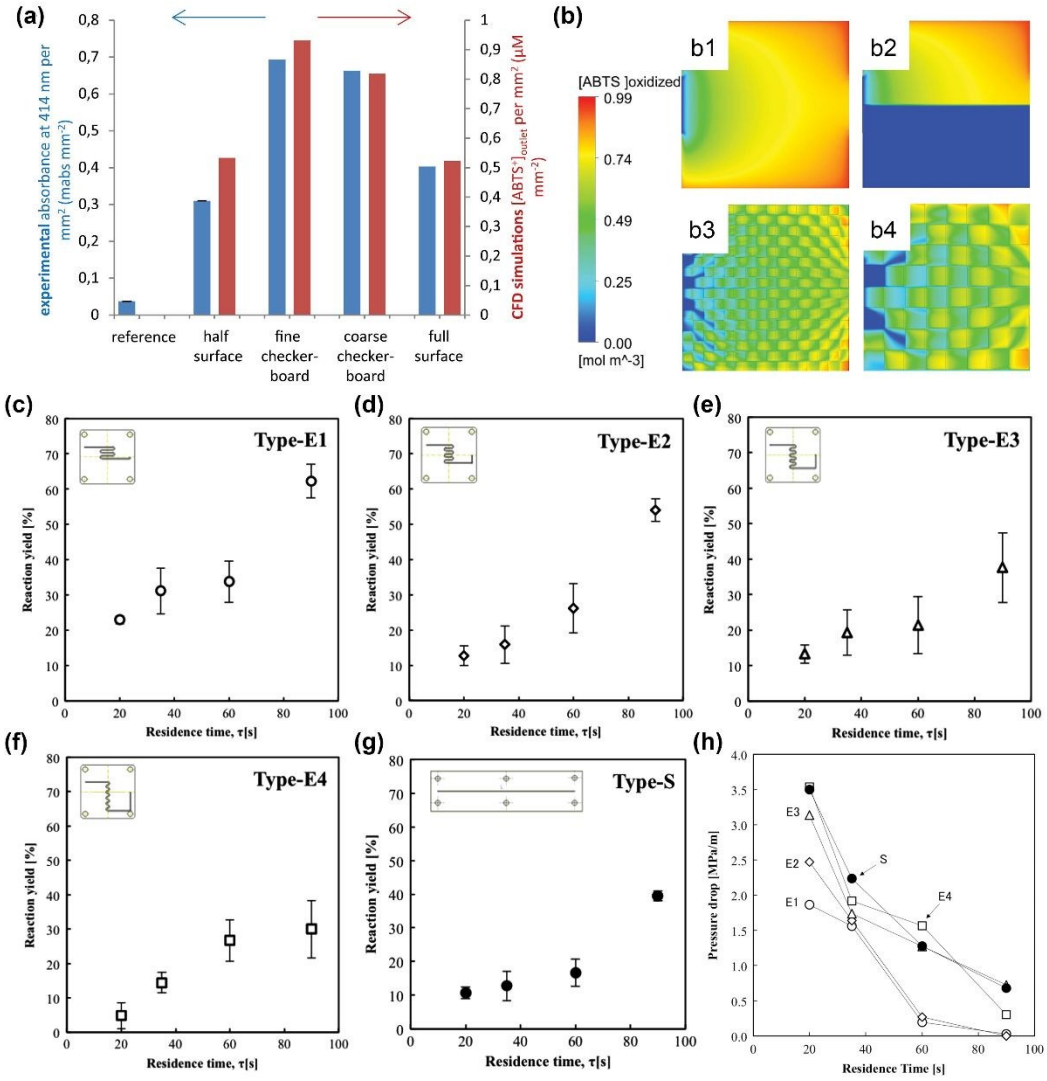


Fig. 2 (a) Comparison of experimentally determined $ABTS^{\bullet+}$ absorbance at 414 nm per $mm^2$ modified area at the reactor outlet in steady state condition (blue) and $ABTS^{\bullet+}$ outlet concentration obtained from CFD simulations in $mM \cdot mm^{-2}$ (red) of various surface patterns: reference (HRP adsorption on non-modified surface, empty squares), half modified surface, coarse checkerboard, fine checkerboard, fully modified surface; (b) Illustration of product concentration on the top surface in the microreactor (in steady state simulations) dimensions using fully modified surface (b1), half modified surface (b2), fine checkerboard structure (b3), coarse checkerboard structure (b4), where red surfaces illustrate a high and blue surfaces a low product concentration. These two

View Article Online
DOI: 10.1039/C9RE00217K

figures were reproduced from Ref. 46 with permission from Elsevier Ltd. (c)-(g) Reaction performance of the prepared five reactors using 0.1% β-lactoglobulin solution as the substrate. (h) Pressure drops of the prepared five reactors. These six figures were reproduced from Ref. 47 with permission from Elsevier Ltd.

## 2.3 Fabrication technologies of microfluidic reactors

The fabrication process of microfluidic reactors includes the microchannel fabrication and the microfluidic chip bonding. The techniques for both steps should be carefully selected by considering the reactors material, the reactors configuration, the fabrication cost and time. For the microchannel fabrication, most techniques are adopted and improved from the MEMS, like photolithography, etching, soft lithography, thermoforming and so on. By contrast, the techniques for the bonding process are generally different from that in MEMS. They may be divided into indirect and direct bonding.

### 2.3.1 Microchannel fabrication

The most widely used technique to fabricate silicon/glass microfluidic channels is photolithography, by which the pattern of a photomask is transferred to the substrate with the assistant of a photosensitive resist. It consists of six steps as shown in Fig. 3. Step 1, the photoresist is spin-coated on a thoroughly cleaned wafer to form a thin layer. Step 2, the wafer is soft baked to remove the solvents in photoresist and improve the adhesion of resist to the wafer. Step 3, the photoresist layer is exposed to the UV light with a photomask. Step 4, the photoresist layer is then immersed in a developer solution to generate a mask for etching after the post exposure baking. Step 5a, the micro-channels are formed on the substrate by etching to remove the unprotected areas of the photoresist mask. Step 6a, the microchannels are ready for use after the residual photoresist

View Article Online
DOI: 10.1039/C9RE00217K

is removed.

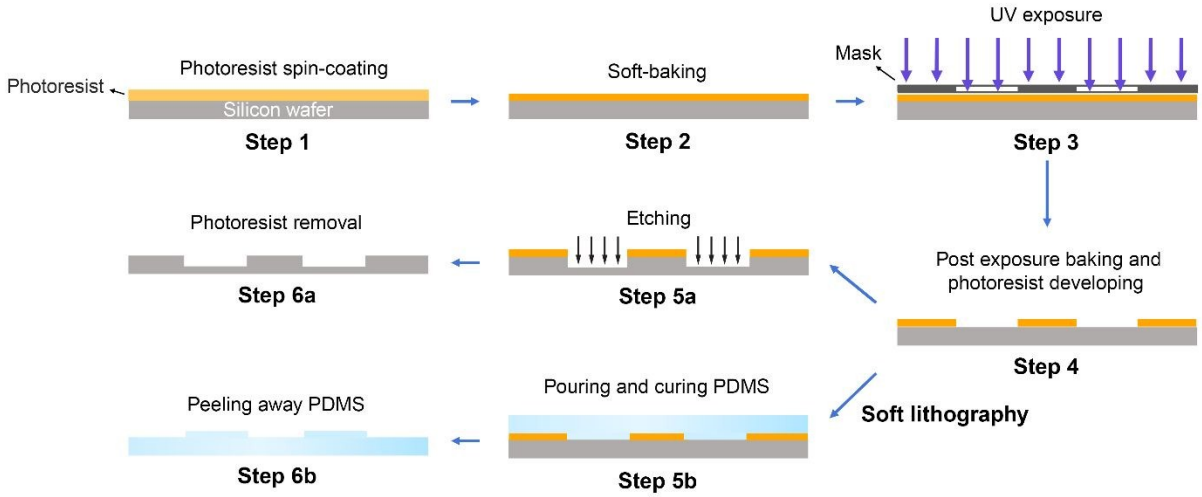


Fig. 3 Process flow of photolithography and soft lithography with PDMS.

As an extension of photolithography, soft lithography is a collection of techniques to fabricate microstructures in a wide range of soft elastomer materials, such as polymers, gels and organic monolayers for the microfluidic applications.[48] Basically, it uses a patterned elastomeric polymer layer as a mask, mold or stamp to emboss, mold or print the pattern to another soft substrate.[49] The patterned elastomeric polymer is usually a layer of PDMS that is fabricated from a solid master produced by photolithography (as shown by Step 5b and 6b in Fig. 3). The basis of soft lithography includes microcontact printing, replica molding, microtransfer molding, micromolding in capillaries and a large number of patterning techniques.[50]

Thermoforming techniques are usually employed to pattern the semi-finished thermoplastic foils by stretching or stamping with pressure and heat.[51,52] The injection molding and hot embossing can also be classified into them. They have the advantages in cost-effective high-volume fabrication and high frequency manufacturing.[44] However, the thermoforming techniques are less precise to control the aspect ratio than the lithography techniques.[53]

View Article Online
DOI: 10.1039/C9RE00217K



### 2.3.2 Bonding process

The bonding process is a very critical step following the microchannel fabrication, by which the microfluidic reactors are sealed to form the enclosed fluid paths.[54,55] The indirect bonding use an adhesive layer to bring the two substrates together, Epoxy, adhesive tape, or chemical reagents are generally the candidates. The additional layer may affect the chemical, optical and mechanical properties of the substrate materials. In contrast, the direct bonding method, such as oxygen plasma bonding, allows the sealing without any additional materials to the interface.[56] As a result, the sidewalls of microchannels would be homogeneous with the substrates. The effect of bonding process to the properties of the substrates should be carefully considered when selecting the bonding method. Moreover, some other key parameters, such as the bond strength, surface chemistry, materials properties and fabrication costs, should also be taken into account.

### 2.3.3 Three-dimensional printing for microfluidics

PDMS and soft lithography make the fabrication of microfluidics easy and cost-effective.[57] However, the limitations of these traditional techniques for microfluidics in large scale, mass-production and three-dimensional (3D) structures fabrication are still inescapable. Recently, the application of 3D printing in microscale fabrication has attracted great interest in microfluidics due to the rapid development of commercial 3D printers.[58] 3D printing has the obvious advantages in rapidly fabricating complex 3D microfluidic devices in a single step from a computer model.[59] The most widely used 3D printing techniques include selective laser sintering (SLS), fused deposition modeling (FDM), photopolymer inkjet printing, laminated object manufacturing (LOM), and stereolithography (SL).[57] Nevertheless, fabricating microfluidic devices using 3D printing technology still needs attentions in some aspects, like the precise control at small scale, cost reduction and the adaptability of the 3D printers to different materials.[60,61]

View Article Online
DOI: 10.1039/C9RE00217K



# 3. Internal structure designs of microfluidic channel

The amount and the activity of the immobilized enzyme in the microfluidic chip greatly impact the biocatalytic reaction rate. And the internal structure of microfluidic channels would strongly affect these two factors by adjusting the surface-area-to-volume (SAV) ratio of the microchannel and the diffusion pressure of the solution passing through it. Generally, the internal structures of the μ-IMERs are classified into three types: wall-coated type, monolithic type and packed-bed type (Fig. 4). The comparison of the properties of the three types of the microchannels is presented in Table 1.

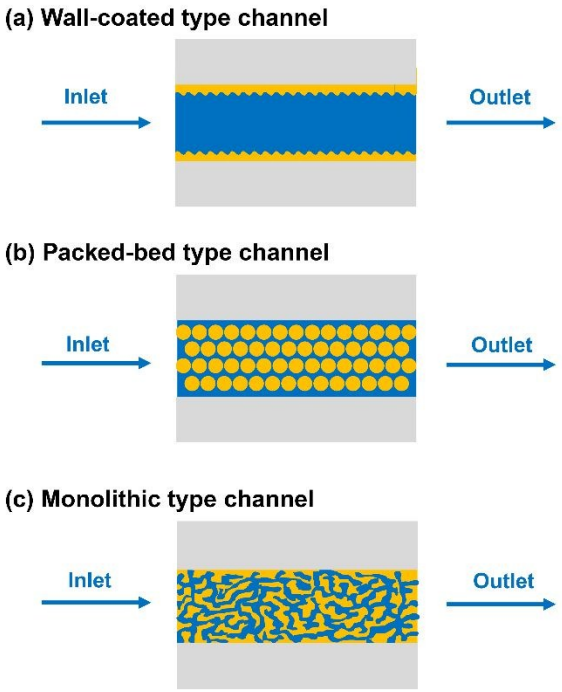


Fig. 4 Typical designs for the internal structure of microfluidic channels.

View Article Online
DOI: 10.1039/C9RE00217K



Table 1 Comparison of the properties of different microchannel types

| ***Microchannel type*** | ***Wall-coated*** | ***Packed-bed*** | ***Monolithic*** |
|---|---|---|---|
| *SAV ratio* | Small | **Large** | **Large** |
| *Pressure drops* | **Low** | High | **Low** |
| *Diffusion length* | Large | **Small** | **Small** |
| *Heat transfer* | **Large** | Small | Moderate |
| *Mechanical stability* | **High** | Low | Moderate |

## 3.1 Wall-coated type channel

For the wall-coated type μ-IMERs (Fig. 4a), the enzyme is directly immobilized onto the inner wall surface of the microchannel.[62-64] Notably, the available surface areas of the microfluidic walls are quite limited, resulting in low enzyme-loading capacity. In addition, the substrate diffusion path is relatively large in this case and then leading to low biocatalytic conversion rate. Researchers are dedicated to increase the SAV ratio of microchannel, therefore the enzyme loading capacity would be enlarged. One efficient method is to modify the inner wall with some biocompatible nanostructured materials like dopamine,[65] gold nanoparticles,[66] graphene, [67,68] graphene oxide,[69,70] nanosprings,[71] or MXene.[72]

Recently, Valikhani *et al*. designed a borosilicate microchannel with silica nanosprings attached on the surface for the immobilization of sucrose phosphorylase (Fig. 5a).[71] It was demonstrated that the enzyme-loading amount was increased by an order of magnitude or more as compared to that of the enzyme loaded on the uncoated microchannel walls. Moreover, the nanosprings microreactor also showed an enhanced conversion efficiency on the synthesis of α-glucose 1-phosphate and an improved reusability and stability compared with the plain

View Article Online
DOI: 10.1039/C9RE00217K



microreactor. Another feasible solution to increase the active enzyme-loading amount is to multiple the immobilization layers, which is also defined as the layer-by-layer (LBL) assembly approach.[34,35,73-75] A representative work was conducted by Bi *et al*. who alternatively absorbed polyethyleneimine (PEI) and *Candida antarctica* lipase B (CAL-b) on the microreactor surface (Fig. 5b).[35] The lipase loading was enlarged as the number of layers was increased. It reached saturation at the 8th layer. The microreactor was also demonstrated to have a high conversion efficiency and an excellent stability to produce wax ester.

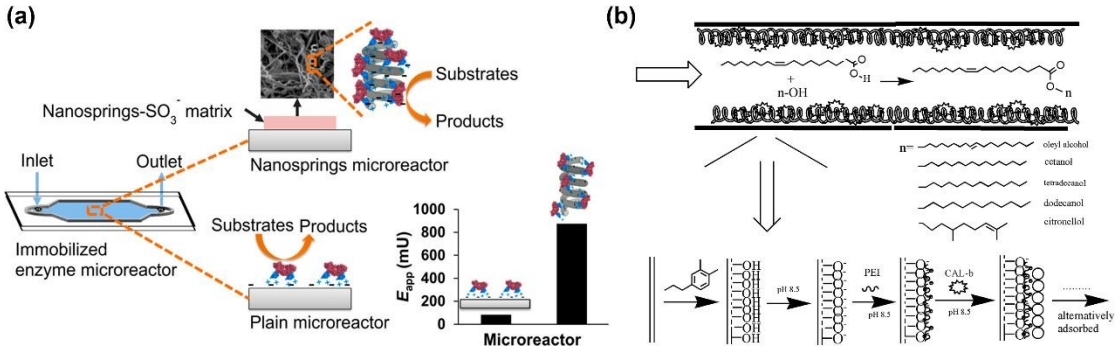


Fig. 5 Examples of wall-coated microchannels for enzyme immobilization. (a) Schematic of the sucrose phosphorylase immobilized on the nanosprings microreactor with enhanced enzyme activity. Reprinted with permission from Ref. 71. Copyright 2017 American Chemistry Society. (b) Process of immobilization of CAL-b based on self-oxidation of dopamine and LBL method. Long chains with positive charges represent PEI, and the circles represents the lipase. Reproduced from Ref. 35 with permission from The Royal Society of Chemistry.

## 3.2 Packed-bed type channel

Even though many methods have been developed to increase the SAV ratio of the wall-coated type μ-IMERs, the enhancement room is very small. In order to maximize the space utilization of the size-limited channels and therefore maximizing the enzyme-loading amount, enzymes are

View Article Online
DOI: 10.1039/C9RE00217K



designed to be immobilized on polymeric or inorganic particles. The enzyme-immobilized particles are then packed into the microchannel of the μ-IMERs, which is regarded as the packed-bed type channel (Fig. 4b). The higher SAV ratios of the packed-bed channel also ensures relatively shorter diffusion distance for substrate to enzyme compared with the wall-coated channel.[76,77] Many polymeric particles are already commercially available for the packing.[77-80] Some inorganic materials like glass,[81,82] silica,[83] and $Fe_2O_3$ microparticles[84-86] have also been explored. These packed-bed type μ-IMERs can be fabricated easily and present an extremely high enzyme-loading capacity.

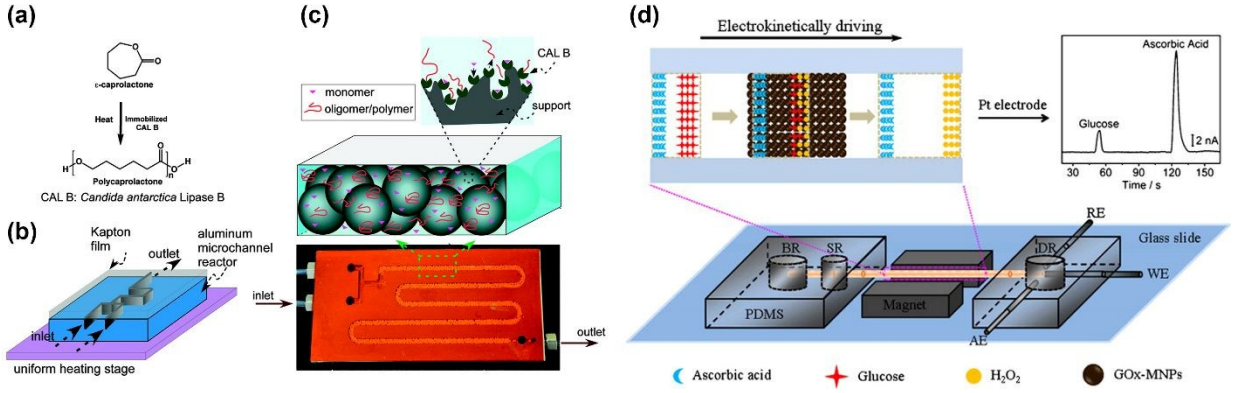


Fig. 6 Examples of packed-bed microchannels for enzyme immobilization. (a) Reaction scheme for ring-opening polymerization of ε-caprolactone to polycaprolactone. (b) Schematic of the microreactor setup. (c) Image shows the photograph of a typical microreactor used in this study. CAL-b immobilized solid beads (macroporous polymethyl methacrylate) were filled in the channel. These three figures were reprinted with permission from Ref. 78. Copyright 2011 American Chemistry Society. (d) Scheme representation of the construction and analytical procedure of glucose oxidase (GOx)-magnetic nanoparticles (MNPs)-microfluidic device (MD). BR, buffer reservoir; SR, sample reservoir; DR, detection reservoir; WE, working electrode; RE, reference electrode; AE, auxiliary electrode. Reproduced from Ref. 86 with permission from Elsevier Ltd.

View Article Online
DOI: 10.1039/C9RE00217K



Kundu *et al*. designed a microreactor packed with commercially available mesoporous PMMA beads where CAL-b was physically immobilized to study the polymerization of polycaprolactone from ε-caprolactone in the continuous mode (Fig. 6a-c).[78] It was demonstrated that faster polymerization and higher molecular mass were obtained in the microreactors as compared to that in the batch reactors. Another example is the packing of GOx modified MNPs in microfluidic channels for the electrochemical detection of glucose (Fig. 6d).[86] The performance of the MD could be optimized by changing the packing length of the MNPs, which was hard to achieve in other types of devices. The device also showed good reproducibility, favorable stability and great potential in glucose detection without the need for the pretreatment of serum samples. However, due to the densely packed particles, the fluid passing through the channel is hard to control and the heat transfer inside the channel is very limited.[87] Moreover, there may be huge pressure drops when the substrate solution flows along the channel. These may have negative impact on the enzyme activity.

## 3.3 Monolithic type channel

To overcome the drawbacks of the packed-bed type channel, such as high pressure drop, limited heat transfer and the possible leakage at high flow rates, the monolithic type channel (Fig. 4c) is developed. In such a case, the channel is filled by the monolithic material with interconnected meso- or micro- porous structure. This structure exhibits high void fractions, making it easy for the fluid flowing. Consequently, relatively higher flow rates, lower pressure drop, and higher productivities as compared to the packed-bed type channel are obtained in monoliths.[1,88-90] Higher backpressure can facilitate the rapid diffusion of substrate to immobilized enzyme. As a result, the enzyme activity is increased, which is reflected from the increase in turnover number ($k_{cat}$) and decrease in Michaelis constant ($K_M$).[91] It also possesses the advantages of high mechanical

View Article Online
DOI: 10.1039/C9RE00217K



durability and reduced diffusion path length over the wall-coated type channel. Qiao *et al*. immobilized L-asparaginase (L-Asnase) in both the monolithic microreactor and the coating reactor (i. e., the wall-coated type) by the same immobilization method.[92] Fig. 7a-d show the SEM of the monolithic and coating microreactors. The monolithic microreactor was demonstrated to have a lower $K_M$ than the coating microreactor, showing that a better affinity between the substrate and the enzyme can be obtained in the monolithic structures as a result of the lower diffusion path length in monoliths (Fig. 7e). However, a higher maximal velocity was observed in the coating microreactor due to its relatively lower flow pressure.

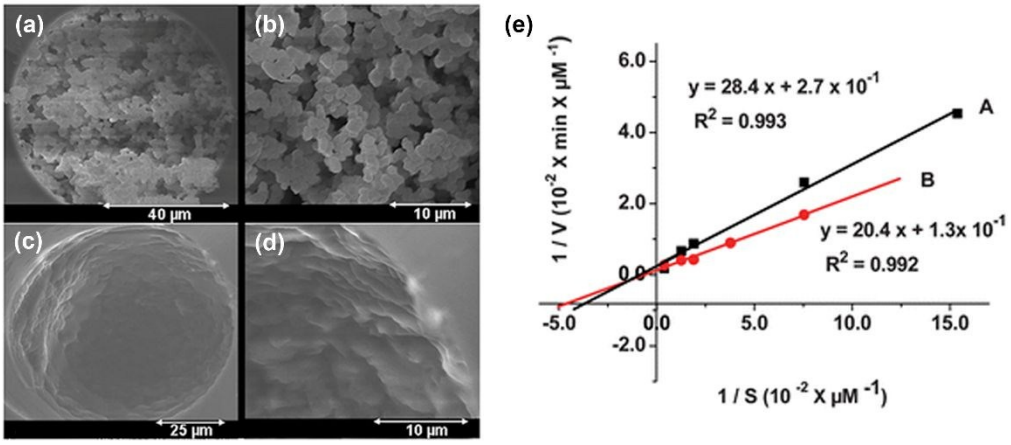


Fig. 7 SEM of monolithic and coating in capillary: (a, b) monolithic, (c, d) coating. (e) Lineweaver-Burk plots for L-Asnase immobilized in the monolithic (A, ■) and coating (B, ●) enzymatic microreactors. Reproduced from Ref. 92 with permission from The Royal Society of Chemistry.

The monolithic materials can be organic,[93-97] inorganic[98-101] or hybrid.[66,102-104] The selection should be careful for different enzyme immobilizations and different reaction environments. Generally, the organic monoliths are copolymerized from many monomers and sometimes one of the monomers is the enzyme. They usually have good biocompatibility and pH resistance but may be damaged by some organic solvents. An example is the immobilization of amylase in the PVA

View Article Online
DOI: 10.1039/C9RE00217K



foams by mixing the amylase solution with the PVA solution before they were put in a cylindrical sample case for freeze drying.[94] The amylase-immobilized microreactor was demonstrated to successfully conduct continuous starch hydrolysis reactions over 8 days. For the inorganic monoliths, silica-based monoliths are most widely used due to their high binding capacity, great biocompatibility, chemical and thermal stability, and easily functionalization.[105] But compared with the organic polymer monoliths, the preparation of inorganic monoliths is relatively difficult.[106] Therefore, the monoliths used for enzyme immobilization are hybrids of organic and inorganic materials in most of the time. For example, Ma *et al*. developed an organic-inorganic hybrid silica monolith with immobilized trypsin and demonstrated its excellent enzymatic activity and long-term stability in proteome analysis.[102] However, there is still the possibility that the pores are blocked, leading to the non-uniform permeability along the channel. And the fabrication of monolithic materials is usually time consuming and poorly reproducible. Each the internal structure has its own advantages and disadvantages. All the aspects should be taken into account as much as possible when designing. Attentions should especially be paid to the economy, sustainability and green chemistry for industrial application.

# 4. Enzyme immobilization techniques

Since Nillson and Griffin firstly reported that invertase remained its activity after physical adsorption to charcoal in 1916,[107] various enzyme immobilization techniques have been developed and studied. Most of these techniques can be directly used for enzyme immobilizations in microfluidic chips for biocatalysis. The combination of enzyme immobilization and microfluidic chips provides the advantages of high stability and reusability, high enzyme to substrate ratio, and rapid catalytic reactions.[108] Basically, the techniques of

View Article Online
DOI: 10.1039/C9RE00217K



enzyme immobilization in microfluidic chips can be classified into two types: surface binding and encapsulation, as shown in Fig. 8. The inner surfaces of microfluidic reactors can offer the support for enzyme immobilization when surface binding technique are used. Besides, the microchannels with special microstructures can entrap relatively larger structures, then the encapsulation of enzyme can be applied. For the surface binding method, it is usually subdivided into non-covalent binding and covalent binding. Non-covalent binding includes non-specific physical adsorption, ionic bonding, his-tag/metal binding, and affinity binding.[3,109] While the covalent binding is to immobilize enzymes on the surface via covalent forces between certain functional groups, like amino, carboxyl, hydroxyl or sulfhydryl groups.[110] As for the encapsulation immobilization, enzymes are confined in small spaces built by polymeric networks, membranes, or nanochannels. Different immobilization methods have different advantages as well as disadvantages (see Table 2). Therefore, careful consideration should be given before one immobilization strategy is adopted. Some representative examples of μ-IMERs for biocatalysis are summarized in Table 3.

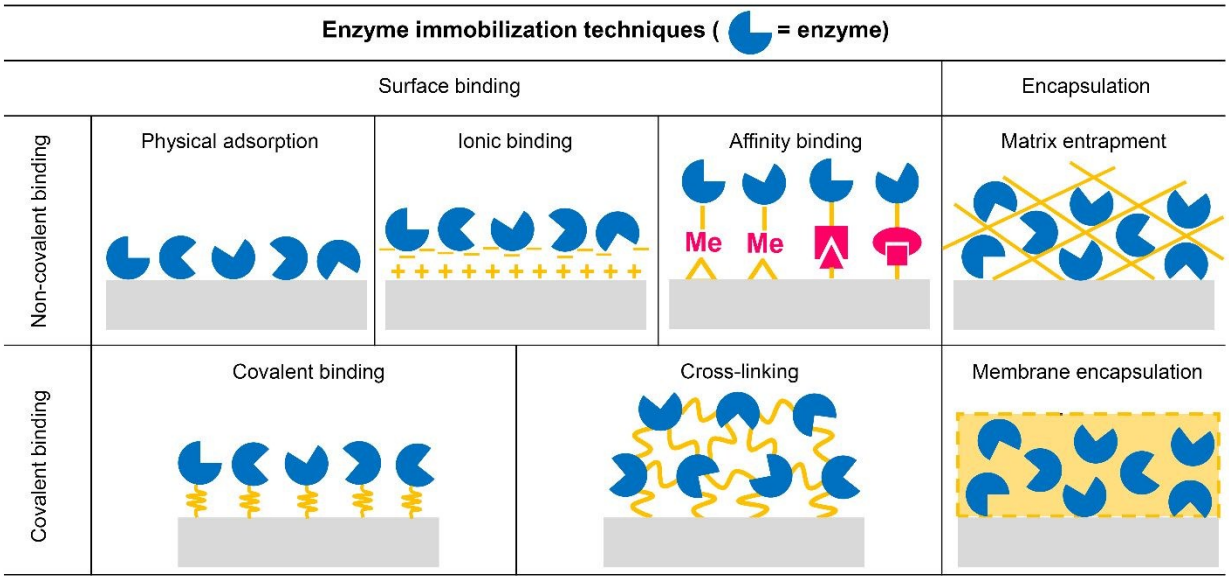

View Article Online
DOI: 10.1039/C9RE00217K

Fig. 8 Different enzyme immobilization techniques.

Table 2 Characteristics comparison of different enzyme immobilization techniques.

| ***Characteristics*** | ***Physical adsorption*** | ***Ionic binding*** | ***Affinity binding*** | ***Covalent binding*** | ***Cross-linking*** | ***Entrapment and encapsulation*** |
|---|---|---|---|---|---|---|
| *Preparation* | **Simple** | **Simple** | Moderate | Difficult | Moderate | Difficult |
| *Cost* | **Low** | **Low** | Moderate | High | Moderate | Moderate |
| *Applicability* | **Wide** | **Wide** | **Wide** | Selective | Selective | **Wide** |
| *Binding force* | Weak | Moderate | Moderate | **Strong** | **Strong** | **Strong** |
| *Stability* | Low | Moderate | Moderate | **High** | **High** | **High** |
| *Enzyme leakage* | Yes | Possible | Possible | **No** | **No** | Possible |
| *Enzyme activity* | Moderate | **High** | **High** | Low | Low | Moderate |
| *Protection from microbial* | No | No | No | No | Possible | **Yes** |
| *Diffusional limitation* | **Low** | **Low** | **Low** | **Low** | Moderate | High |

Table 3 Summary of recent μ-IMERs studies.

| **Immobilization techniques** | **Enzyme** | **Platform** | **Biocatalysis performance** | **Refs.** |
|---|---|---|---|---|
| Physcial immobilization | CAL-b | Macroporous PMMA microbeads packed aluminum microreactor | Faster polymerization and higher molecular mass | 78 |
| Ionic binding | Angiotensin-converting enzyme | Fused silica capillary column | High activity, stability, reusability, renewability and reduced costs. | 111 |

View Article Online
DOI: 10.1039/C9RE00217K



| | | | | |
|---|---|---|---|---|
| | Sucrose phosphorylase | Nanosprings-coated Borosilicate glass | 10-fold activity enhancement, 11-fold operational stability increase, 85% conversion rate retaining after 840 reactor cycles | 71 |
| Layer-by-layer ionic binding | Trypsin | Wall-coated PET microfluidic chip | Short digestion time and small volume of protein samples, a potential solution for low-level protein analysis | 34 |
| | CAL-b | PTFE open-tubular microreactor | Production efficiency reached to 95% within 35 mins, 83% initial activity retained after 144 hours usage | 35 |
| His-tag/Ni-NTA binding | PikC hydroxylase | Agarose beads packed PDMS microfluidic reactor | High enzyme loading and conversion rate | 112 |
| | Transketolase | Wall-coated PMMA microfluidic chip | The 1-step-immobilization method without the pre-amination of PMMA surface showed higher specific activity. | 113 |
| Streptavidin/biotin | ALP, GOx and HRP | Phospholipid bilayer-coated PDMS microchannels and borosilicate microcapillary tubes | The feasibility of using the microchannels to obtain kinetic data and the potential application for multistep chemical synthesis were demonstrated. | 114 |
| | HRP and β-galactosidase | PDMS microchip reactor packed with commercial microbeads | Similar kinetic analysis results were obtained in the microfluidic-based assays as that obtained in solution, reduced cost, reagent economy and increased throughput were | 80 |

View Article Online
DOI: 10.1039/C9RE00217K



| | | | | |
|---|---|---|---|---|
| | | | observed. | |
| | ALP, Gox and HRP | Protein coated PDMS/glass microchannel | Photoimmobilization of multiple, well-defined enzymes were developed for both single-enzyme and multi-enzyme systems. | 115 |
| DNA directed immobilization | CAL-b and HRP | Fused silica capillaries with polymer coated | High reusability and renewability, the reaction time available for glucose oxidase could be independently and modularly varied by the distance between two enzymes | 116 |
| Covalent binding | Trypsin | Porous polymer monolithic microfluidic capillaries and chips | Very short digestion time compared to the traditional approach and great potential for broader application in various protein mapping | 97 |
| | GOx | Magnetic nanoparticles packed microreactor | Low detection limit of glucose, hign reproducibility and storage stability, avaliability of direct detectio of serum samples | 86 |
| | β-Gal and GOx | Au coated PDMS microfluidic chip | 5 times of the reaction yield could be obtained if the gap distance decreased from 100 to 50 μm | 117 |
| Encapsulation | Trypsin | PMMA microchip filled with sol-gel | Analytic time was shortened and operation stability was increased, digestion of protein with multiple cleavage sits and separation of digest | 118 |

View Article Online
DOI: 10.1039/C9RE00217K



| | | | | |
|---|---|---|---|---|
| | | | fragments are applicable. | |
| | Trypsin | Titania and alumina sol-gel based PDMS microfluidic reactors | Short digestion time and increased operation stability | 119 |
| | Lipase | Mesoporous silica coated PDMS/glass microreactor | Higher activity compared to that in batch system | 120 |
| Cross-linking | Aminoacylase | Wall-coated PTFE microtubes | Higher stability against heat and organic solvents, applicable to various enzymes with low isoelectric points. | 36 |
| Cross-linking/encapsulation | ALP and urease | PDMS microfluidic device with PEG-based hydrogel structures | enzyme-catalyzed reactions were able to reach 90% conversion within 10min. | 121 |

## 4.1 Surface binding

### 4.1.1 Non-specific physical adsorption

The non-specific physical adsorption is the simplest and most convenient approach. The interactions between enzyme and support are non-specific forces such as van der Waals forces, hydrogen bonds and hydrophobic interactions.[27] Compared with other immobilization methods, the conditions for physical adsorption are more mild and no chemical modification is needed during the procedures. Therefore, the chances of conformational change caused by the immobilization are very little. In addition, the physical adsorption is usually reversible, makes it possible for the same device to be reused by washing and reloading new enzymes. This indicates a relatively low fabrication cost for large-scale production.[3]

However, non-specific forces are generally very weak and highly dependent on environmental and surface conditions. As a result, the enzymes are easy to fall off from the surface

View Article Online
DOI: 10.1039/C9RE00217K



especially in fluidic systems or high ionic and pH solutions. This would cause to the contamination of reaction systems and the reduction of enzyme activity. In addition, since the enzymes adsorbed on the support are randomly oriented, the activity of enzyme can also be affected by the hindering of active sites to the support due to the randomly orientation after adsorption. Moreover, some other problems, like diffusion resistance, denaturation of enzyme, and overloading, could also cause the enzyme activity loss when physical adsorption is adopted.[122] Therefore, the combination of other immobilization methods and the adsorption method is usually applied to overcome these shortcomings and to enhance the enzyme activity, stability and the overall efficiency.

#### 4.1.1 Ionic binding

The ionic binding is achieved by the electrostatic interactions between the positively and negatively charged functional groups of the enzymes and the supports. The amount of immobilized enzyme can be well manipulated if the pH of solution is controlled below the isoelectric point of the enzyme and above that of the support material.[105]

Generally, the ionic binding is stronger than non-specific physical adsorption, which would subsequently guarantee a higher enzyme stability and reusability. But the ionic binding is highly dependent on the environmental pH and ionic strength. This may affect the enzyme loading amount and the pH stability of enzymes. Therefore, the selection of suitable chemicals with appropriate isoelectric point is the focus of this method. In biochemistry, the typical positively charged functional groups are protonated amine ($NH_3^+$) and quaternary ammonium cations ($NR_4^+$). The negatively charged functional groups are usually carboxylic acid ($-COO^-$) and sulfonic acid ($-RSO_3^-$).[27] PEI is one popular polycation which has multiple cation groups with strong anion exchange capacity for enzyme immobilization by ionic binding.[35,123-126] Some other polycations have also been used for the ionic binding, such as chitosan,[34,73] hexadimethrine bromide

View Article Online
DOI: 10.1039/C9RE00217K



(HDB)[111,127] and poly (diallyl dimethylammonium chloride) (PDDA).[128,129] Sometimes, polyanions like alginate,[123,124] hyaluronic acid (HA),[34,73] poly(Lys),[36] and functionalized graphene oxide[70] are also employed to form multi-layers to stabilize the immobilization and to increase the enzyme-loading amount.

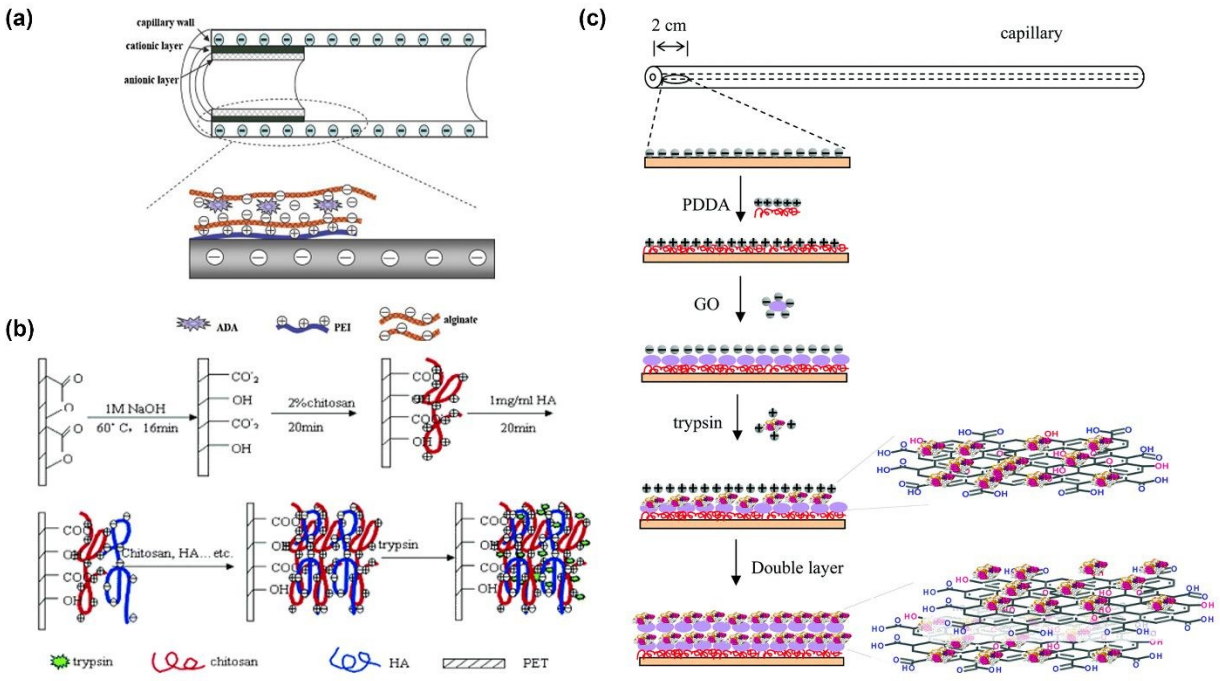


Fig. 9 Schematic representations of enzyme immobilization by ionic binding via different polycations and polyanions. (a) Adenosine deaminase (ADA) immobilization of by PEI and alginate. Reproduced from Ref. 123 with permission of Elsevier Ltd. (b) Trypsin immobilization by HA and chitosan. Reprinted with permission from Ref. 34. Copyright 2006 American Chemistry Society. (c) Trypsin immobilization by PDDA and negatively charged graphene oxide. Reproduced from Ref. 70 with permission from The Royal Society of Chemistry.

Some schematic representations of enzyme immobilization by ionic binding via different polycations and polyanions are shown in Fig. 9. The reversibility of the enzyme immobilization by ionic binding is also an important advantage over other immobilization methods. The support

View Article Online
DOI: 10.1039/C9RE00217K

surface can be washed without damages by simply changing the ionic strength of the environment. Then new enzymes can be immobilized to the same support. In this way, reuse of the microfluidic chip is available, thereby saving the labor and the cost.

### 4.1.2 Affinity binding

The affinity binding enables to immobilize enzyme on the support via some specific ligands, such as his-tag/metal binding, avidin/biotin binding, DNA-directed immobilization and antigen/antibody binding. Therefore, it can ensure the high loading amount and enzyme stability. Sometimes, more than one affinity binding methods are adopted into one device to improve the binding efficiency and the loading amount. In non-specific enzyme immobilization methods like physical adsorption or covalent binding, the orientation of enzymes is hard to control. Then the activities of enzyme are likely to lose due to the block of active sites and the conformation change. While in the affinity binding, the orientation of enzymes is controlled well to expose the active sites to the substrate, which helps to maintain the activities. The affinity binding can also be reversed by pH or temperature change or some special chemical treatments to favor the reusability of the microreactors. However, the enzymes often need to be decorated with some tags genetically or chemically to prepare for the immobilization. This step makes it more complicated and costly for affinity binding as compared to the other methods.

#### A) His-tag/metal binding

Metal binding needs enzymes and supports to be bonded together by the coordination with metals in between of them. Generally, highly active, stable and specific immobilized enzymes can be obtained by this method.[130-132] The enzyme loading amount by this method is also usually higher than that by other methods.[112,131] In such case, polyhistidine linkers are genetically tagged to the

View Article Online
DOI: 10.1039/C9RE00217K



enzyme and then connected to the nitrilotriacetic acid (NTA) attached on the support for the enzyme immobilization. Recently, Kulsharova *et al*. immobilized transketolase (TK) in PMMA microfluidic devices by two methods of the his-tag/Nickel-NTA interactions: the 1-step-immobilization method (see Fig. 10a) and the 3-step-immobilization method.[113] The device fabricated by the 1-step-immobilization method presented higher specific activity and reusability than the 3-step method. The 1-step method also required fewer chemicals and less time. Moreover, it was also demonstrated that the his-tag/Ni binding had high reversibility, facilitating the reuse of the microreactor.[133]

However, this method also suffers many intrinsic drawbacks. Sometimes this method is not easily reproducible due to the nonuniform adsorption sites and the metal ion leakage.[134] Therefore, it is usually combined with covalent bonding or cross-linking to get a more stable formation of adsorption sites and chelation.

View Article Online
DOI: 10.1039/C9RE00217K



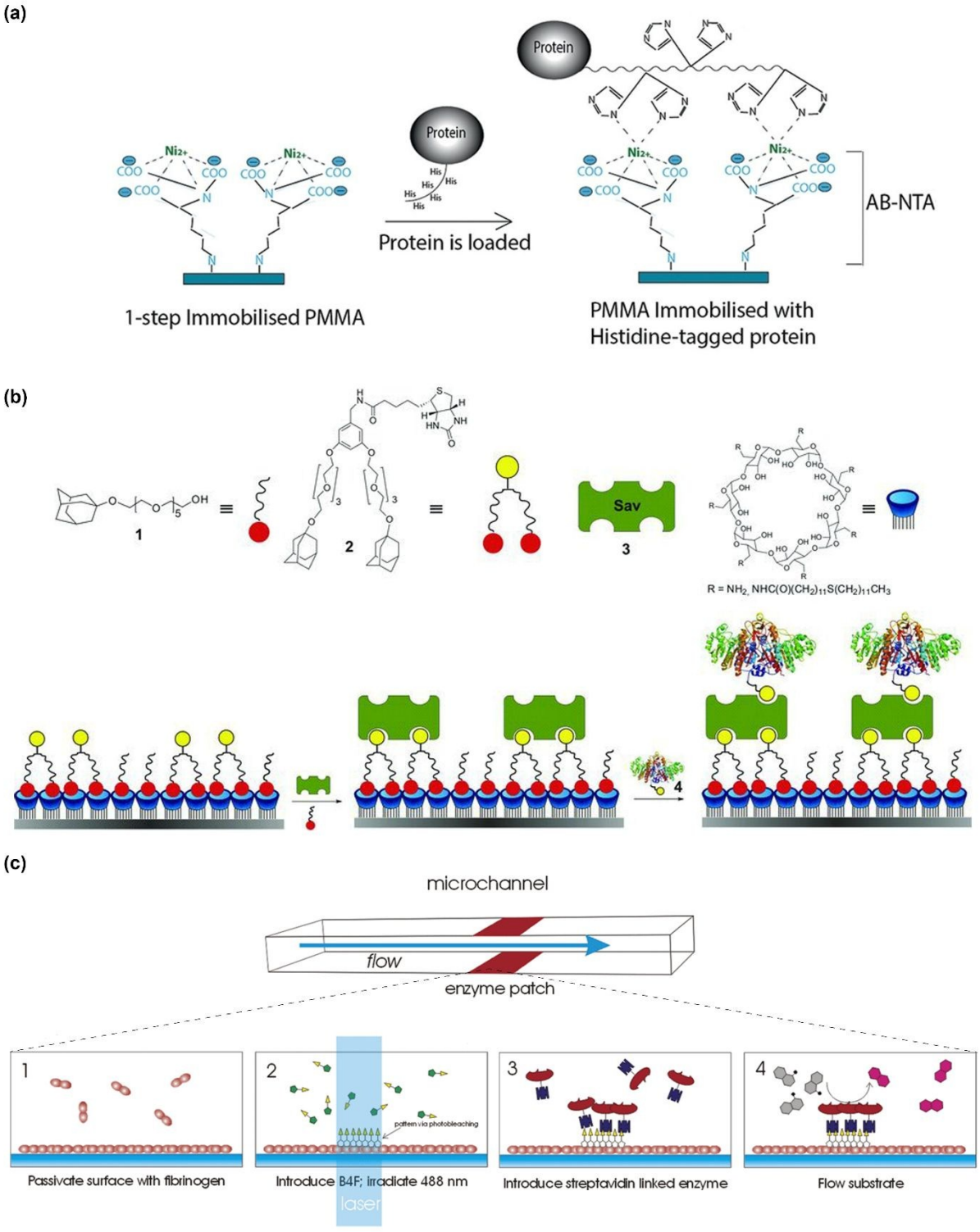


Fig. 10 Schematic representations of enzyme immobilization by His-tag/metal binding (a) Diagram of enzyme immobilized by the His-tag/Ni-NTA binding; Reproduced from Ref. 113 with

View Article Online
DOI: 10.1039/C9RE00217K



permission from Elsevier Ltd. (b) Chemical structures of the building blocks and scheme for the step-wise assembly process. Ethylene glycol-based mono-adamantyl linker (b1) for minimizing the non-specific protein adsorption, biotinylated bisadamantyl linker (b2) for the first assembly step and streptavidin (b3) as the second assembly step. Biotinylated ALP (bt-ALP, 4) is immobilized onto these streptavidin-biotin surfaces. Reproduced with permission from Ref. 137. Copyright 2004 American Chemistry Society. (c) Schematic diagram of the photo-immobilization process. (Top) Enzyme patches are formed on the top and bottom of a microchannel using the following procedure: (c1) Passivation of the surface with a fibrinogen monolayer is followed by (c2) biotin-4-fluorescein surface attachment. This is accomplished by photobleaching with a 488-nm laser line. (c3) Next, the binding of streptavidin-linked enzymes that can be exploited to immobilize catalysts and (c4) to monitor reaction processes on-chip. Reproduced from Ref. 115 with permission from John Wiley & Sons, Inc.

## B) Avidin/biotin binding

The avidin/biotin binding is one of the most popular affinity binding with high affinity and specificity. The interaction is regarded as the strongest non-covalent interaction[135] having the advantages of rapid fabrication and insensitivity to pH, temperature, proteolysis and denaturing agents.[84,114,136] Moreover, the avidin or biotin can be easily modified by other chemicals, enabling more effective enzyme immobilization or some interesting functions.[115,137]

Gonzá lez-Campo *et al*. developed a supramolecular platform with the combination of orthogonal supramolecular interactions of host (β-cyclodextrin)–guest (adamantane) and biotin–Streptavidin interactions for site-selectively immobilization of enzyme in microchannel (Fig. 10b).[137] The microfluidic chip with supramolecular platform was demonstrated to present great

View Article Online
DOI: 10.1039/C9RE00217K



reproducibility and reusability in enzymatic reactions when calf intestine alkaline phosphatase (ALP) was used as the model enzyme. The site-selectively immobilized ALP was also able to maintain the comparable activity in other environments (free in solution or immobilization by other methods). Holden *et al.* also presented a work for the photo immobilization of multiple enzymes in PDMS/glass microfluidic channels by site-specific immobilization (Fig. 10c).[115] Biotin-linked dye solution was used to immobilize the streptavidin linked enzyme on the selected photopatterning positions. The patterning of enzymes in sequence inside the microfluidic channels were achieved by photobleaching instead of valves.

## C) DNA-directed immobilization

The DNA-directed immobilization (DDI) is based on the Waston-Crick paring mechanism between the single-strand DNA (ssDNA) attached on enzymes and the complementary DNA (cDNA) attached on the supports. The attachment of ssDNA to enzyme is usually accomplished by covalent binding or avidin/biotin binding.[116,138,139] Generally, the binding by DDI is more stable and robust than other methods, therefore presenting high immobilization efficiency and site-specificity. The DDI method is superior to others mainly lies in the ability of precisely control the relative positions of different enzymes,[19] which is critical to the cascaded enzymatic reactions.

### 4.1.3 Covalent binding

The covalent binding is formed by the chemical reaction between functional groups on the surface of support and the amino acid residues of the enzyme. The most commonly used covalent bonds are based on the Schiff or carbodiimide chemistries as shown in Fig. 11a.[10] Since the covalent binding always offers the strongest bond between the enzyme and the support, the enzyme usually behaves high stability, great reusability and strong resistance to extreme environment. However,

View Article Online
DOI: 10.1039/C9RE00217K



conformation change and activity reduction of enzyme may sometimes occur after immobilization. Moreover, the orientation of enzyme is harder to control as compared to the specific immobilization, resulting in the decrease of reaction rate. Nevertheless, blocking the active sites of enzyme with a competitive inhibitor or substrate before immobilization may alleviate this problem.

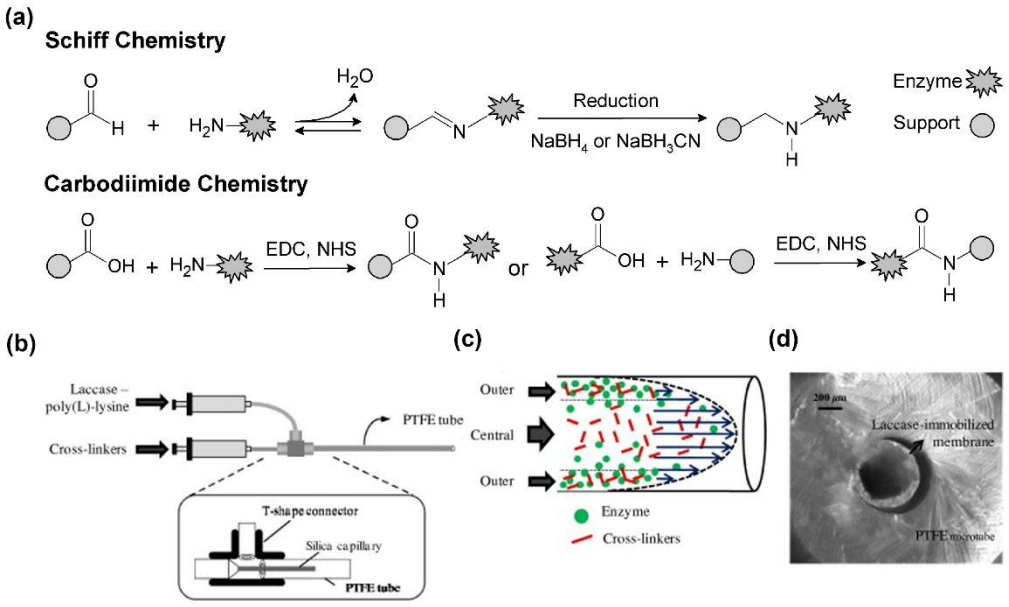


Fig. 11 Covalent binding for enzyme immobilization. (a) Commonly used covalent bonds: mechanisms of the Schiff chemistry and the Carbodiimide chemistry; Reproduced from Ref. 10 with permission from Elsevier Ltd. (b) Preparation of laccase-immobilized membrane on the inner wall of a PTFE microtube; (c) Parabolic velocity profile characteristic of the laminar flow inside the microtube, and (d) confocal acquisition of the sectional view of the laccase-immobilized microreactor (dry state). These three figures were reproduced from Ref. 140 with permission from Elsevier Ltd.

Typically, only one layer of the covalently immobilized enzyme can be formed on the surface of support. Then the loading amount would be very limited. Therefore, a cross-linker may be

View Article Online
DOI: 10.1039/C9RE00217K



utilized to form an enzyme polymerization for its increase. Lloret *et al*. prepared a laccase-immobilized microreactor by the formation of an enzyme-polymeric membrane on the inner wall of microtubes (Fig. 11b-d).[140] The membrane was formed by the cross-linking polymerization reaction between laccase and the cross-linkers (paraformaldehyde and glutaraldehyde). The microreactor with cross-linked laccase not only presented important biotransformation efficiency compared with conventional bioreactors, but also exhibited excellent pH, temperature, inactivating agent, storage and long-term stabilities.

## 4.2 Encapsulation

The encapsulation of enzyme is defined as enzyme being entrapped inside a small space that allows the substrates and products to pass through but retains the enzyme. It mainly includes matrix entrapment and membrane encapsulation, as shown in Fig. 8. For the matrix entrapment, enzymes are entrapped into a matrix, which is usually formed by polymers (like alginate[123,124] and PEG hydrogels[121,141,142]) or some inorganic materials (like Titania[119] and silica sol-gels[98,118,143]). When a semipermeable membrane, like the hollow fiber[144] or microencapsulate[145], is used to encapsulate the enzymes, it is classified as membrane encapsulation. Compared with the physical adsorption, the entrapment method is more stable and can immobilize a larger amount of enzyme. In addition, the entrapment does not need the chemical modification of enzyme, which not only saves time but also avoids the conformation changes of enzyme. But the slow diffusion of substrate to the enzyme in this case may severely restrict the biocatalytic production. There are also the possibilities of enzyme leakage and enzyme contamination by the matrix. Besides, the microenvironments of the matrix are hard to control, which may lead to the reduction of enzyme activity and stability. However, there is a great opportunity to reduce the impact of these problems by carefully choosing the polymer materials with proper modification and by adjusting the pore size or capsule size.

View Article Online
DOI: 10.1039/C9RE00217K

Moreover, the capsules can imitate the multicompartment structures of cellular architectures to encapsulate enzymes in controllable number, type and spatial arrangement, thus maintaining or even enhancing the overall catalytic activity.[146,147]

Mizukami developed a microreactor containing lipase encapsulated in folded-sheet mesoporous (FSM) silicas with two different pore diameters (Fig. 12a and b).[120] The FSM with larger diameter (~7 nm) (FSM7) indicated a higher enzyme loading amount than the FSM with a smaller diameter (~4 nm) (FSM4). The two types of lipase-FSMs were loaded in the microreactors for the hydrolysis of a triglyceride, both presented a higher enzyme activity than the batch reaction. The results also revealed that the enzymatic activity in the lipase-FSM7 was slightly higher than that in lipase-FSM4. This may be attributed to the larger pore size of FSM7 that facilitates the access of the substrate to the encapsulated enzyme. Blanchette *et al*. entrapped active particulate methane monooxygenase (pMMO) and associated lipids in a PEG-based hydrogel (Fig. 12c).[141] The hybrid materials were then suspended between gas and liquid reservoirs in a flow-through reactor (Fig. 12d). With this configuration, methane/air gas mixture and NADH could be introduced into the reactor constantly while continuously removing and collecting methanol in buffer. The native conformation and physiological activity of pMMO are 100% retained by this encapsulation method. In addition, the strategy enables the reuse and continuous use of pMMO. Besides, this method allows the facile fabrication of the immobilization structures in 3D structures from micro to millimeter scales, which guarantees a higher loading of pMMO compared with the surface immobilization.

View Article Online
DOI: 10.1039/C9RE00217K



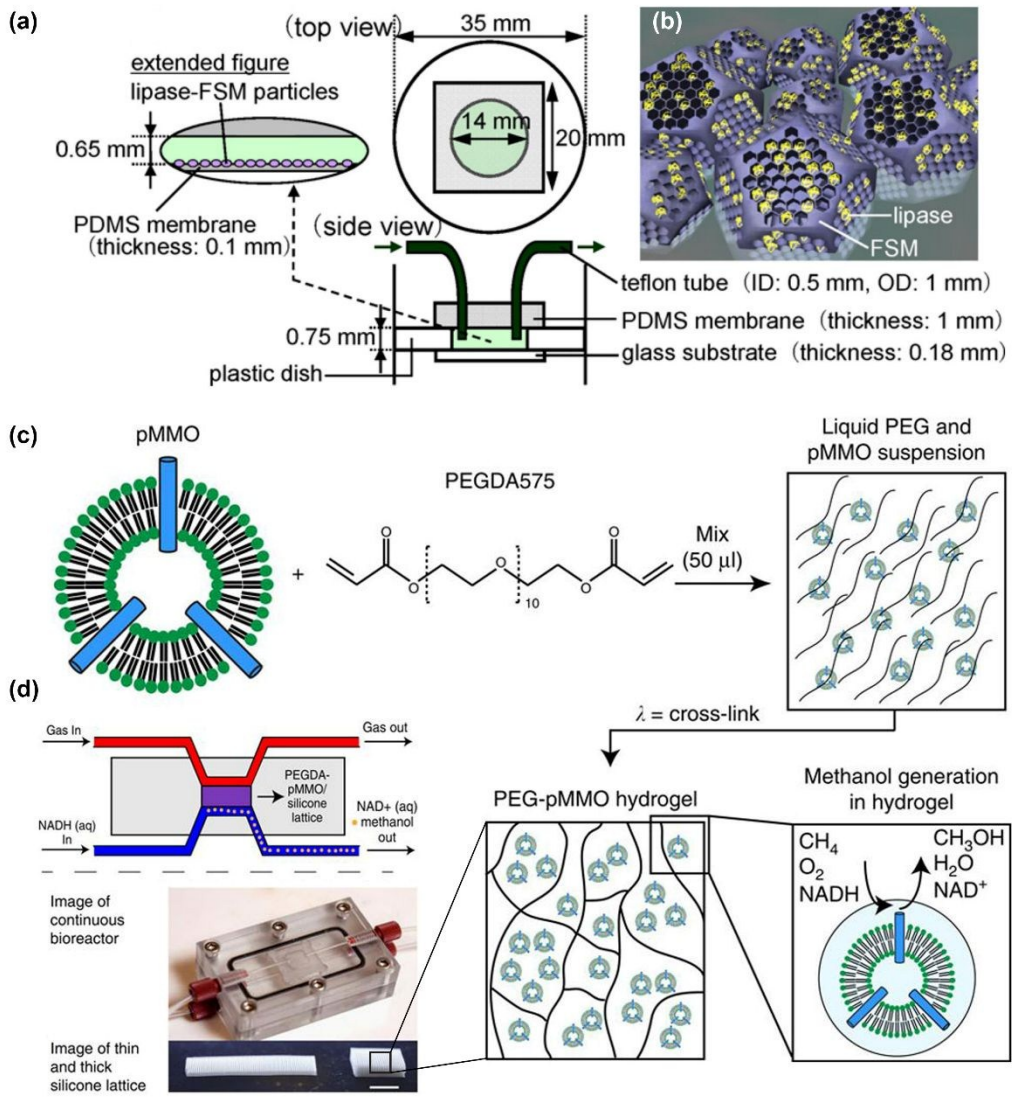


Fig. 12 Examples of enzyme immobilization by encapsulation. (a) Schematic illustrations of the microreactor with immobilized lipase–nanoporous material (FSM) composite particles; (b) Lipase molecules encapsulated in the FSM pores; These two figures were reproduced from Ref. 120 with permission from Elsevier Ltd. (c) Schematic of PEG-pMMO hydrogel fabrication. Membrane-bound pMMO is mixed with PEGDA 575 and photoinitiator and exposed to ultraviolet light to crosslink the material. (d) Schematic and image of the flow-through bioreactor and the two (thin and thick) silicone lattice structures used to support the PEG-pMMO hydrogel membrane (scale bar, 1 cm); These two figures were reproduced from Ref. 141 with permission from Springer

View Article Online
DOI: 10.1039/C9RE00217K



Nature.

## 5. Multi-enzymes systems

Most natural biocatalytic reactions are catalyzed by more than one enzyme. Tremendous efforts have been devoted to immobilizing multiple enzymes in one microfluidic reactor to artificially construct the various biocatalytic reactions in nature.[77,96,117,138,142,148-150] The methods for multi-enzymes immobilization are based on those for single enzyme immobilization. But careful considerations should be taken to maintain the activities and catalytic efficiencies of all enzymes according to the structures and optimal environments of different enzymes. One major issue for multi-enzymes immobilization is the control of their relative spatial positions in one reactor, though it is much easier for microfluidic reactors as compared to that for the batch reactors. The well controlled spatial positions would probably promote the increase in reaction rate and catalytic efficiency. The unwanted side reactions and the accumulation of inhibitors or reactive intermediates may also be avoided.[151-155]

Multiple enzymes can be immobilized in one pot,[142,149] sequentially[116,117,138] or layer by layer.[156] Heo *et al*. packed glucose oxidase (GOx) and horseradish peroxidase (HRP) bearing microbeads into microfluidic reactors with different spatial distances as shown in Fig. 13a.[157] Reactor I packed the microbeads co-immobilizing both GOx and HRP. Reactor II had the GOx-immobilized microbeads packed in front of the HRP-immobilized microbeads. In Reactor III, the GOx and HRP immobilized microbeads are mixed and packed. It was demonstrated that a better overall reaction efficiency was obtained in Reactor I than the other two reactors. The increased efficiency due to the decreased enzyme distance can be attributed to the reduced diffusional loss of intermediate product ($H_2O_2$) and the prevention of the accumulation of inhibitor. Another work

View Article Online
DOI: 10.1039/C9RE00217K



presented by Wu *et al*. investigated the distance for multi-enzyme immobilization in micrometers and arrived at a similar result.[117] β-galactosidase and glucose oxidase were immobilized on two separated gold films patterned in one microfluidic channel, as shown in Fig. 13b. The highest conversion efficiency of the cascaded reaction was obtained when the two enzymes were in minimum distance (50 μm). Even though the spatial positions of enzymes are easy to control by separating microchannels into multiple areas, they are still not very close to each other like the case in the natural cascaded systems.[158] Researcher then pay their attentions to the combination of microfluidic reactors and DDI, by which more precise spatial control can be obtained for the reaction efficiency enhancement. It has been demonstrated that when the enzymes GOx and HRP were immobilized via DNA origami tiles at 10 nm from each other, an increase of more than 15-fold in the overall cascade activity was observed as compared to the free enzymes as shown in Fig. 13c.[159] The reason of the activity increase was suggested to be the efficient transport of the reaction intermediate ($H_2O_2$) between the two enzymes.

The sequential order is also very important for the overall reaction efficiency in multi-enzyme systems. As shown in Fig. 13d, three enzymes (INV, GOx and HRP) were spatially immobilized by a photopatterning method on porous polymer monoliths within microfluidic devices.[96] The three-enzyme system was used to perform a sequential reaction with sucrose hydrolyzed to glucose and fructose by INV in the first step. Then GOx would oxidize glucose to gluconolactone and hydrogen peroxide, which was following oxidized by HRP to Amplex Red. Among all the six possible arrangements of the three enzymes, the correct sequential order of catalyst (INV-GOx-HRP) resulted in the largest resorufin fluorescence by more than 3-fold. This demonstrates that the correct enzyme order is critical for the reaction efficiency in the multi-enzyme immobilized microfluidic system.

View Article Online
DOI: 10.1039/C9RE00217K





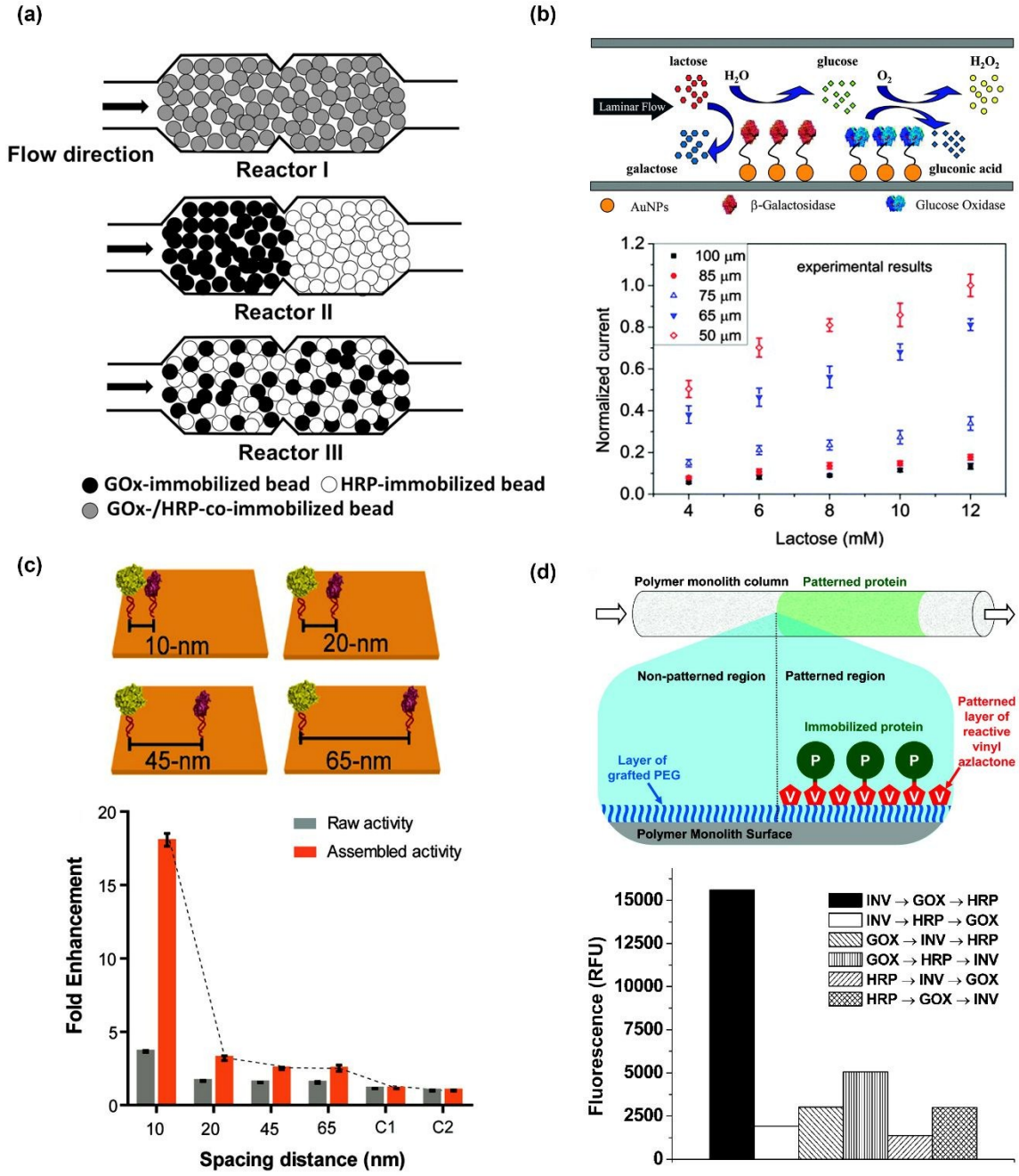


Fig. 13 Examples of enzyme immobilization in multi-enzyme systems. (a) Diagrams of three different configurations of microfluidic reactors. In reactor I, GOx and HRP were co-immobilized on a single set of beads. In reactor II, GOx-immobilized beads and HRP immobilized beads were loading sequentially. In reactor III, the two beads were mixed in the reactor. Reprinted with

View Article Online
DOI: 10.1039/C9RE00217K



permission from Ref. 157. Copyright 2014 Japan Society for Analytical Chemistry. (b) Schematic of enzyme cascade reaction confined in a microchannel. β-galactosidase and glucose oxidase were assembled on the Au-films with controllable distances (up). Graph of the normalized response currents of $H_2O_2$ as a function of the concentration of lactose with different gap distances in the experiment (down). Reproduced from Ref. 117 with permission from the PCCP Owner Societies. (c) Rectangular DNA origami tiles with assembled GOx (yellow) and HRP (purple) pairs spacing from 10 to 65 nm (up). Enhancement of the activity of the enzyme pairs on DNA nanostructures compared to free enzyme in solution (down). The largest enhancement factor was observed when the inter-enzyme distance was decreased to 10 nm, as analyzed with d-glucose, $ABTS_2$–(2,2'-azinobis(3-ethylbenzothiazoline-6-sulfonate)) and $O_2$ as substrates at pH 7.2. $C_1$ and $C_2$ refer to the tiles without nucleic acid and free enzymes, respectively. Reprinted with permission from Ref. 159. Copyright 2012 American Chemistry Society. (d) Schematic representation of the microfluidic set-up used for performing the sequential synthesis with a three-enzyme system: invertase (INV), GOX and HRP. Enzymes are immobilized to the surface of a polymer monolith in patterned regions within a microfluidic channel. Poly(ethylene glycol) (PEG) is grafted to the surface of the polymer monolith to prevent nonspecific protein adsorption. Vinyl azlactone is photopatterned onto the PEG surface and activates the surface for protein immobilization (up). Product fluorescence measured with each possible arrangement of the three enzymes are indicated in the figure legend (down). The substrate solution consisted of 10 mg/mL sucrose, 100 μmol/L Amplex Red (10-acetyl-3,7-dihydroxyphenoxazine), and 1.0% (v/v) dimethyl sulfoxide (DMSO) in 50 mmol/L phosphate buffer, pH 7.50; pure oxygen was bubbled through this solution for 15 min prior to use. The flow rate was 0.10 μL/min. Reprinted with permission from Ref. 96. Copyright 2007 American Chemistry Society.

View Article Online
DOI: 10.1039/C9RE00217K



# 6. Scalability of microfluidic reactor

The application of microfluidic reactors to biocatalysis owns many inherent benefits, such as rapid heat transfer, precise reaction control, and the capability for continuous and integrated operation. Microfluidic reactors are also advantageous in the robust structures, the capacity and the ease of scalability for mass production.[17,160] These are particularly attractive to the synthesis of petrochemicals, active pharmaceutical ingredients or value-added materials in industry. Generally, two methods of scaling the microfluidic reactors have been widely discussed: scaling up (increasing the characteristic dimensions of the channel) and scaling out (using parallel reactor systems or stacking up multiple microreactors), as shown in Fig. 14.

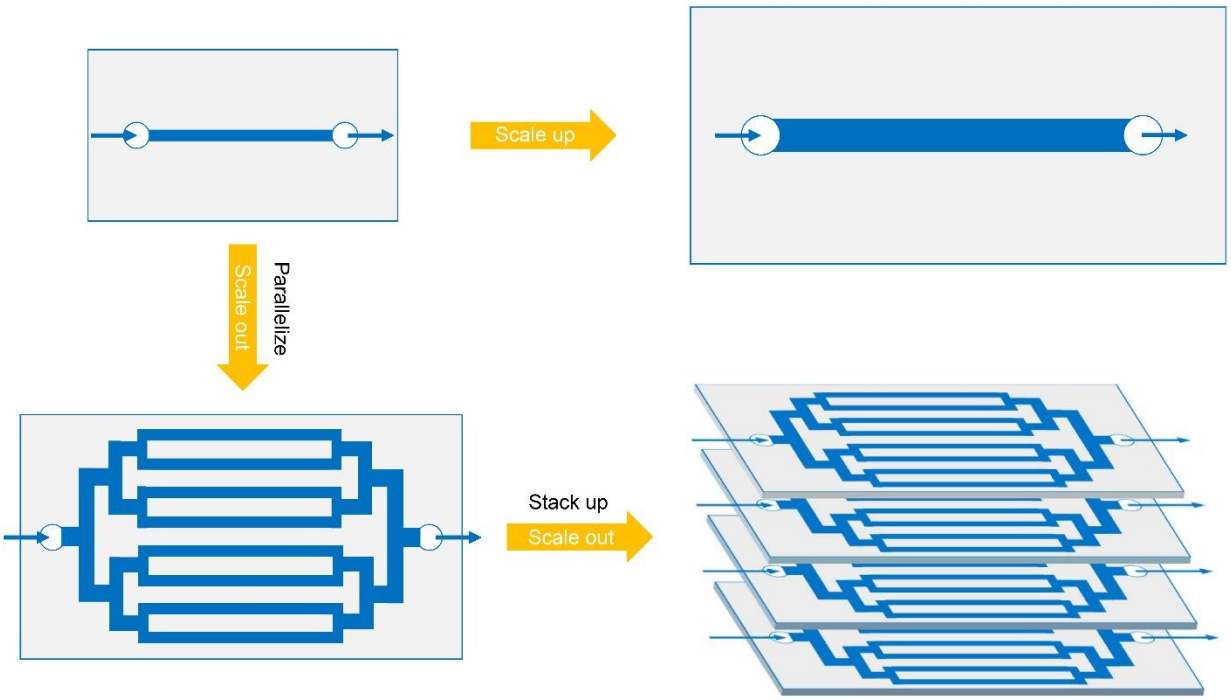


Fig. 14 Illustration of the concept of scaling the microreactors up and out. Scaling up means increasing the characteristic dimensions of the channel. For scaling out, the parallel microchannels are used or multiple microreactors are stacked up.

View Article Online
DOI: 10.1039/C9RE00217K



Many reviews have comprehensively discussed the microreactor design and scale-up concept.[20,161-163] The principle for scaling up a single-channel reactor is presented as the relationship between its characteristic dimension and the mixing and heat transfer characteristics. Some studies also use mathematical models comprising the reaction kinetics and the flow dynamics to optimize the reaction conditions and reactor designs for the scaling up.[164-167] As for the scaling out, it has the advantages over scaling up in remaining the reactions performed in each reactors the same at any level.[168,169] Generally, the scaling out is practicable by designing a multiple-channel reactor with only one pump and heating apparatus.[170] Uniform flow distribution should be ensured as well as the same residence time in all microchannels when designing the manifold structures. Amador studied an analytical model based on the electrical resistance networks for two manifold structures to describe the flow in each microchannel.[171] Based on this model, the design and fabrication of scale-out microreactors applied to different operation conditions is feasible.

View Article Online
DOI: 10.1039/C9RE00217K



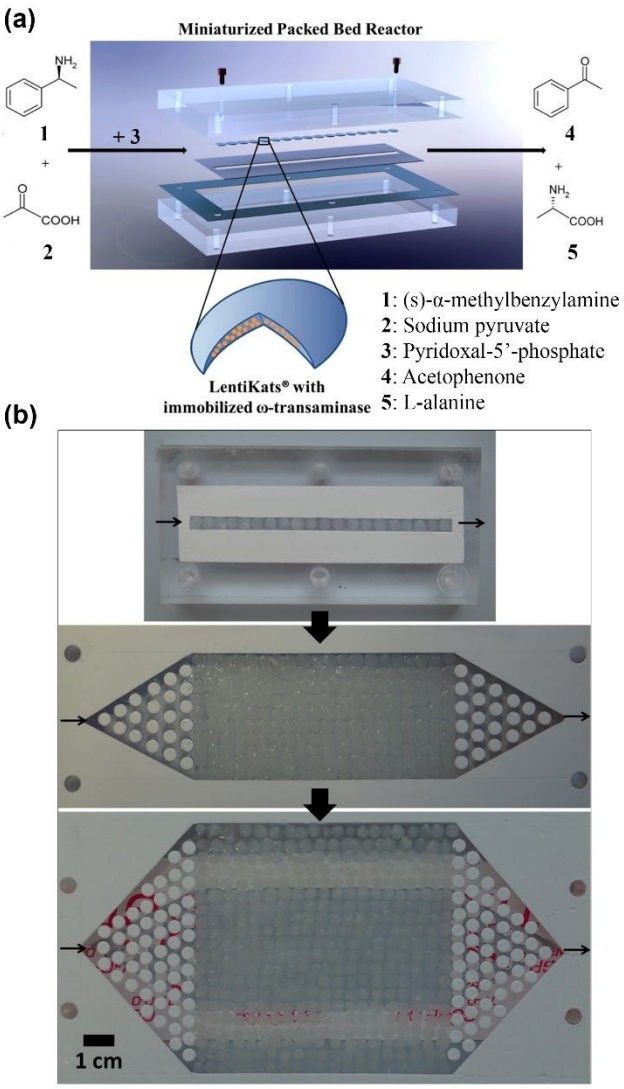


Fig. 15 (a) Diagram of the miniaturized packed bed reactor (MPBR) packing LentiKats® with immobilized $\omega$-transaminase for continuous enzymatic process. (b) MPBRs presenting the scale-up in channel width. The MPBRs from up to down is cca. 4 mm wide rectangular channel, hexagonal channel (rectangular part is cca. 40 mm wide) with triangular inlet and outlet parts containing pillars and hexagonal channel (rectangular part is cca. 80 mm wide) with triangular inlet and outlet parts containing pillars. Reproduce from Ref. 145 with the permission of Elsevier Ltd.

Recently, Bajić et al. conducted a scale-up study on a two-plate miniaturized packed-bed

View Article Online
DOI: 10.1039/C9RE00217K



reactor (MPBR) in which LentiKats® (lens-shaped PVA particles) encapsulated with *ω*-transaminase (*ω*-TA) were uniformly or randomly packed (as shown in Fig. 15a).[145] The MPBR was used for the synthesis of acetophenone (ACP) and L-alanine (L-ALA) from *(S)*-α-methylbenzylamine (*(S)*-α-MBA) and sodium pyruvate (PYR). Productivity was evaluated by increasing the capacity of the reactor from microliter to milliliter by adjusting the length, width and depth of the channel. Fig. 15b was three representative reactors by scaling-up in width. The results reveled that increasing the length and width would increase the productivity. While increasing the depth would reduce it. Here, the flow distribution that encourages the accessibility of the substrates to the immobilized enzyme is the key to increase the productivity when increasing the reactor size. This study provided a simple but efficient guide for scaling-up. But for commercial-scale production, a combination of scaling up and scaling out may be the best option.[170] In addition, for a continuous reaction, the production amount can be increased by simply increasing the operation time without changing the reaction conditions. Therefore, the large-scale production can be achieved in a simple, green and cost-effective way.

As one of the earliest application of immobilized enzyme for biocatalysis in continuous flow, Liu *et al.* reported the continuous production of uridine diphosphate galactose (UDP-Gal) by circulating galactose (Gal), uracil monophosphate (UMP) and polyphosphate (polyP) through a column packed with seven enzymes-immobilized agarose beads, as shown in Fig. 16a.[172] The enzymes were immobilized by histidine tags on the nickel agarose beads. Small-scale reactions on mini Pasteur pipette columns were carried out first to optimize the reaction conditions. Then the packed-bed column was scaled up to gram-scale to meet the practical biosynthesis. Compared with the solution reaction, the on-column reaction results in higher product yields in long-time reaction (50% of the UMP converted into UDP-Gal in 48 h) compared with the solution reactions, which

View Article Online
DOI: 10.1039/C9RE00217K



thanks to the reusability and stability of the immobilized enzyme (Fig. 16b). This continuous synthesis of UDP-Gal can help to alleviate the difficulties in the production of sugar nucleotides, which is important for the synthesis of pharmaceutically valuable oligosaccharides. Orsat *et al.* reported a continuous acylation process to produce monoacylated Vitamin A precursors from 1,6-diol by immobilized lipase Chirazyme L2-C2 (lipase B from Candida antarctica).[173] A laboratory-scale fixed-bed reactor was firstly utilized to investigate the optimal reaction conditions with >99% yield and >97% selectivity with the yield of 49 g $day^{-1}$. Then kilogram-scale reactor was accordingly prepared with a throughput of 1.6 kg $day^{-1}$ over one hundred days. The production of Vitamin A precursors is environment-friendly, robust and sustainable as a result of the recyclable chemicals. Some recent studies have also demonstrated the successful scale-up of the μ-IMERs for biocatalytic synthesis.[174-176]

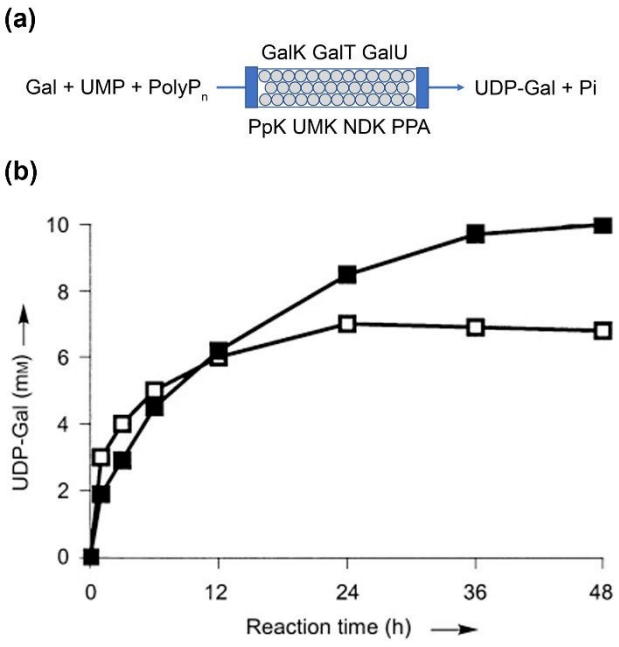


Fig. 16 (a) Biosynthesis of UDP-Gal in the continuous packed-bed column with seven immobilized enzymes. The staring materials are Gal, UMP and polyP. Seven enzymes are used for the catalysis: galactokinase (GalK, EC 2.7.1.6), galactose 1-phosphate uridyltransferase (GalT, EC 2.7.7.10),

View Article Online
DOI: 10.1039/C9RE00217K



UDP-glucose pyrophosphorylase (GalU, EC 2.7.7.9), polyphosphate kinase (PpK, EC 2.7.4.1), uridine monophosphate kinase (UMK, EC 2.7.4.14), nucleotide diphosphate kinase (NDK, EC 2.7.4.6), and pyrophosphatase (PPA, EC 3.6.1.1). UDP-Gal and two phosphate (pi) were formed in the end. (b) Time course of UDP-Gal production. The reaction on the super-bead column (200 mL, filled squares) was performed with UMP and Gal (20 mM each), polyP (2 % (w/v)), ATP and glucose-1-phosphate (2 mM each). About 50 % UMP was converted into UDP-Gal in 48 h. Reaction in the solution with the purified enzymes (50 mL, open squares) used the same reaction composition. About 35 % UMP was converted in 24 h. Reproduced from Ref. 172 with the permission of John Wiley and Sons.

## 7. Summary and outlooks

Biocatalytic reaction plays an important role in biochemistry thanks to its environmental-friendliness, high efficiency and strong selectivity. However, the most popular biocatalyst, enzymes, often fail to retain the activity and stability in practical applications. The μ-IMERs for the continuous biocatalysis will draw on the benefits of both the microfluidic reactors and the enzyme immobilization techniques for highly efficient, stable, reproducible and continuous biocatalytic reactions in both laboratory and industry. In this review, different factors that affect the production efficiency, stability and reusability in the μ-IMERs are summarized following a top-down strategy.

From the macroscopic aspect, the materials used for microfluidic reactors should be temperature and chemical stable, biocompatible with enzymes, and easy to fabricate. Among all the organic and inorganic materials (glass, silicon, PDMS, PMMA, PC, paper, etc.), PDMS is most popular. It not only meets all the requirements mentioned above, but also has the advantages of

View Article Online
DOI: 10.1039/C9RE00217K

optical transparency, great flexibility, and easy surface modification. Once the fabrication material is chosen, the configuration of microfluidic reactors should also be well designed to make full use of the space for the enzyme loading and the substrate accessing. Fabrication technologies of the microfluidic reactors should also be well chosen according to the materials and the configurations.

From the microscopic aspect, the internal structures of microfluidic reactors should provide a large specific area for the enzyme loading and a short diffusion path to facilitate the affinity of substrate to enzyme. There are three main types of microfluidic channels: wall-coated, packed-bed and monolithic. Generally, the wall-coated channels have the least effects of diffusion resistance on the enzyme activity. However, they usually possess a low specific area and a long diffusion path. Nevertheless, the packed-bed channels have the shortcomings of huge pressure drops. It is also hard to control the fluids and the heat transfer inside the packed-bed channels. For the monolithic channels, some problems, such as non-uniform permeability, poor reproducibility and time-consuming fabrication, may also limit their applications. Overall, each of them has its own strengths and weaknesses, and it is hard to say which one is the best. The design of internal structures should balance every aspect and take into account the used enzyme immobilization technique.

From the nanoscopic aspect, the choice of enzyme immobilization technique is the major factor that affects the overall biocatalytic efficiency of μ-IMERs. For most non-covalent binding methods, they have the advantages of simple fabrication, mild immobilization condition, low chance of conformational change and great reversibility. However, the bonds are generally weak and dependent on pH or ionic strength. For performance improvement, covalent binding is usually employed to provide stronger and more stable interactions for the enzyme and the support. But the enzyme conformation would be changed by using covalent binding, which to some extent may

View Article Online
DOI: 10.1039/C9RE00217K



reduce the activity. Additionally, these non-specific methods can't control the orientation of enzymes, which may cause the block of active sites by the support. This problem may be solved by the site-specific affinity binding which can precisely control the orientation of enzymes and make their active center exposed to the substrate. The site-specific binding also enables a fine positioning of different enzymes in confined spaces, which is noted to play a key role in the multi-enzyme systems. As for the encapsulation, it offers a three-dimensional matrix for enzyme immobilization. Then the enzyme loading amount would be relatively larger than that by those surface binding methods. Nevertheless, there are also some drawbacks like the slow diffusion of substrate to enzyme, the enzyme leakage or the enzyme contamination by the encapsulation materials. On account of these, there is also no perfect immobilization method. More than one strategy is often combined to optimize the activity, stability and reusability of enzymes.

μ-IMERs for continuous biocatalysis can be expanded from laboratory to industry for large amount production by scaling-up and scaling-out if the reaction kinetics and flow dynamics are carefully considered. But there are still difficulties in the wide application due to the numerous and complex issues involved. The challenges also include simplifying the fabrication, increasing the activity and reducing the cost. Some new nanomaterials or nanostructures with high SAV ratios have already been developed as the enzyme immobilization carriers, like molybdenum disulfide,[177,178] halloysite nanotube,[179-181] metal-organic frameworks,[182-184] and so on. But there is still a lack of research in the integration of enzyme-loaded new nanomaterials with the microfluidic reactors for biocatalysis. It is also necessary to increase the type of enzyme used for the μ-IMERs and not limited to the common model enzymes like trypsin, lipase, GOx or HRP. In the future, μ-IMERs with new configuration design and new enzyme immobilization method could be applied to a variety of biocatalyses in both experimental research and industrial production.

View Article Online
DOI: 10.1039/C9RE00217K

## Conflicts of interest

There are no conflicts of interest to declare.

## Acknowledgements

This work is supported by National Science Foundation of China (no. 61377068) and Research Grants Council (RGC) of Hong Kong (N_PolyU505/13, 152184/15E, 152127/17E, 152126/18E and 152219/19E). The authors would like to thank The Hong Kong Polytechnic University for the grants G-YBPR, 4-BCAL, 1-ZE14, 1-ZE27 and 1-ZVGH.

View Article Online
DOI: 10.1039/C9RE00217K



# References


1. L. Tamborini, P. Fernandes, F. Paradisi and F. Molinari, *Trends Biotechnol.*, 2017.
2. A. Schmid, J. Dordick, B. Hauer, A. Kiener, M. Wubbolts and B. Witholt, *Nature*, 2001, **409**, 258-268.
3. X. Zhao, F. Qi, C. Yuan, W. Du and D. Liu, *Renewable Sustainable Energy Rev.*, 2015, **44**, 182-197.
4. D.-M. Liu, J. Chen and Y.-P. Shi, *Trends Anal. Chem.*, 2018.
5. C. Mateo, J. M. Palomo, G. Fernandez-Lorente, J. M. Guisan and R. Fernandez-Lafuente, *Enzyme Microb. Technol.*, 2007, **40**, 1451-1463.
6. S. Cantone, V. Ferrario, L. Corici, C. Ebert, D. Fattor, P. Spizzo and L. Gardossi, *Chem. Soc. Rev.*, 2013, **42**, 6262-6276.
7. A. Liese and L. Hilterhaus, *Chem. Soc. Rev.*, 2013, **42**, 6236-6249.
8. N. R. Mohamad, N. H. C. Marzuki, N. A. Buang, F. Huyop and R. A. Wahab, *Biotechnol. Biotechnol. Equip.*, 2015, **29**, 205-220.
9. R. A. Sheldon and S. van Pelt, *Chem. Soc. Rev.*, 2013, **42**, 6223-6235.
10. K. Meller, M. Szumski and B. Buszewski, *Sens. Actuators, B*, 2016.
11. J. Britton, S. Majumdar and G. A. Weiss, *Chem. Soc. Rev.*, 2018, **47**, 5891-5918.
12. M. P. van der Helm, P. Bracco, H. Busch, K. Szymańska, A. B. Jarzębski and U. Hanefeld, *Catal. Sci. Technol.*, 2019, **9**, 1189-1200.
13. V. Hessel, S. Hardt and H. Löwe, *A Multi‐Faceted, Hierarchic Analysis of Chemical Micro Process Technology: Sections 1.1–1.5*, Wiley Online Library, 2004.
14. E. Wolfgang, H. Volker and L. Holger, *Wiley/VCH, Weinheim*, 2000, 41-84.
15. N. Wang, X. Zhang, Y. Wang, W. Yu and H. L. Chan, *Lab Chip*, 2014, **14**, 1074-1082.
16. Y. Liu and X. Jiang, *Lab Chip*, 2017, **17**, 3960-3978.
17. K. S. Elvira, X. C. i Solvas and R. C. Wootton, *Nat. Chem.*, 2013, **5**, 905.
18. M. B. Plutschack, B. u. Pieber, K. Gilmore and P. H. Seeberger, *Chem. Rev.*, 2017, **117**, 11796-11893.
19. F. Jia, B. Narasimhan and S. Mallapragada, *Biotechnol. Bioeng.*, 2014, **111**, 209-222.
20. J. Zhang, K. Wang, A. R. Teixeira, K. F. Jensen and G. Luo, *Annu. Rev. Chem. Biomol. Eng.*, 2017, **8**, 285-305.
21. R. Porta, M. Benaglia and A. Puglisi, *Org. Process Res. Dev.*, 2015, **20**, 2-25.
22. M. Planchestainer, M. L. Contente, J. Cassidy, F. Molinari, L. Tamborini and F. Paradisi, *Green Chem.*, 2017, **19**, 372-375.
23. M. P. Thompson, I. Peñafiel, S. C. Cosgrove and N. J. Turner, *Org. Process Res. Dev.*, 2018, **23**, 9-18.

View Article Online
DOI: 10.1039/C9RE00217K



24. E. Laurenti and A. dos Santos Vianna Jr, *Biocatalysis*, 2016, **1**, 148-165.
25. S. R. Forrest, B. B. Elmore and J. D. Palmer, *Catal. Today*, 2007, **120**, 30-34.
26. P. Abgrall and A. Gue, *J. Micromech. Microeng.*, 2007, **17**, R15.
27. D. Kim and A. E. Herr, *Biomicrofluidics*, 2013, **7**, 041501.
28. K. F. Lei, in *Microfluidics in Detection Science*, 2014, pp. 1-28.
29. L. M. C. Ferreira, E. T. Da Costa, C. L. Do Lago and L. Angnes, *Biosens. Bioelectron.*, 2013, **47**, 539-544.
30. M. R. F. Cerqueira, D. Grasseschi, R. C. Matos and L. Angnes, *Talanta*, 2014, **126**, 20-26.
31. M. R. F. Cerqueira, M. S. F. Santos, R. C. Matos, I. G. R. Gutz and L. Angnes, *Microchem. J.*, 2015, **118**, 231-237.
32. X. Hu, Y. Dong, Q. He, H. Chen and Z. Zhu, *J. Chromatogr. B*, 2015, **990**, 96-103.
33. D. Ogończyk, P. Jankowski and P. Garstecki, *Lab Chip*, 2012, **12**, 2743-2748.
34. Y. Liu, H. Lu, W. Zhong, P. Song, J. Kong, P. Yang, H. H. Girault and B. Liu, *Anal. Chem.*, 2006, **78**, 801-808.
35. Y. Bi, H. Zhou, H. Jia and P. Wei, *RSC Adv.*, 2017, **7**, 12283-12291.
36. T. Honda, M. Miyazaki, H. Nakamura and H. Maeda, *Adv. Synth. Catal.*, 2006, **348**, 2163-2171.
37. H. Becker and C. Gärtner, *Electrophoresis*, 2000, **21**, 12-26.
38. H. Becker and L. E. Locascio, *Talanta*, 2002, **56**, 267-287.
39. A. Alrifaiy, O. A. Lindahl and K. Ramser, *Polymers*, 2012, **4**, 1349-1398.
40. E. Roy, A. Pallandre, B. Zribi, M. C. Horny, F. D. Delapierre, A. Cattoni, J. Gamby and A. M. Haghiri‐Gosnet, in *Advances in Microfluidics-New Applications in Biology, Energy, and Materials Sciences*, InTech, 2016.
41. J. P. McMullen and K. F. Jensen, *Annu. Rev. Anal. Chem.*, 2010, **3**, 19-42.
42. P. Lisowski and P. K. Zarzycki, *Chromatographia*, 2013, **76**, 1201-1214.
43. F. Figueredo, P. T. Garcia, E. Cortón and W. K. Coltro, *ACS Appl. Mater. Interfaces*, 2015, **8**, 11-15.
44. K. Szymańska, M. Pietrowska, J. Kocurek, K. Maresz, A. Koreniuk, J. Mrowiec-Białoń, P. Widłak, E. Magner and A. Jarzębski, *Chem. Eng. J*, 2016, **287**, 148-154.
45. C. Hoffmann, I. P. R. Grundtvig, J. Thrane, N. Garg, K. V. Gernaey, M. Pinelo, J. M. Woodley, U. Krühne and A. E. Daugaard, *Chem. Eng. J.*, 2018, **332**, 16-23.
46. C. Hoffmann, I. Pereira Rosinha Grundtvig, J. Thrane, N. Garg, K. V. Gernaey, M. Pinelo, J. M. Woodley, U. Krühne and A. E. Daugaard, *Chem. Eng. J*, 2018, **332**, 16-23.
47. K. Nakagawa, A. Tamura and C. Chaiya, *Chem. Eng. Sci.*, 2014, **119**, 22-29.
48. D. B. Weibel, W. R. DiLuzio and G. M. Whitesides, *Nat. Rev. Microbiol.*, 2007, **5**, 209.

View Article Online
DOI: 10.1039/C9RE00217K



49. Y. Xia and G. M. Whitesides, *Angew. Chem., Int. Ed.*, 1998, **37**, 550-575.

50. D. Qin, Y. Xia and G. M. Whitesides, *Nat. Protoc.*, 2010, **5**, 491.

51. M. Focke, D. Kosse, C. Müller, H. Reinecke, R. Zengerle and F. von Stetten, *Lab Chip*, 2010, **10**, 1365-1386.

52. R. Truckenmüller, S. Giselbrecht, C. van Blitterswijk, N. Dambrowsky, E. Gottwald, T. Mappes, A. Rolletschek, V. Saile, C. Trautmann and K.-F. Weibezahn, *Lab Chip*, 2008, **8**, 1570-1579.

53. S.-J. J. Lee and N. Sundararajan, *Microfabrication for microfluidics*, Artech house, 2010.

54. C.-W. Tsao and D. L. DeVoe, *Microfluid. Nanofluid.*, 2009, **6**, 1-16.

55. C. Iliescu, H. Taylor, M. Avram, J. Miao and S. Franssila, *Biomicrofluidics*, 2012, **6**, 016505.

56. C.-W. Tsao, *Micromachines*, 2016, **7**, 225.

57. P. Kim, K. W. Kwon, M. C. Park, S. H. Lee, S. M. Kim and K. Y. Suh, *BioChip J.*, 2008, **2**, 1-11.

58. E. Peris, O. Okafor, E. Kulcinskaja, R. Goodridge, S. V. Luis, E. Garcia-Verdugo, E. O'Reilly and V. Sans, *Green Chem.*, 2017, **19**, 5345-5349.

59. S. Waheed, J. M. Cabot, N. P. Macdonald, T. Lewis, R. M. Guijt, B. Paull and M. C. Breadmore, *Lab Chip*, 2016, **16**, 1993-2013.

60. A. K. Au, W. Huynh, L. F. Horowitz and A. Folch, *Angew. Chem., Int. Ed.*, 2016, **55**, 3862-3881.

61. D. Pranzo, P. Larizza, D. Filippini and G. Percoco, *Micromachines*, 2018, **9**, 374.

62. J. S. Lee, S. H. Lee, J. H. Kim and C. B. Park, *Lab Chip*, 2011, **11**, 2309-2311.

63. A. Küchler, J. N. Bleich, B. Sebastian, P. S. Dittrich and P. Walde, *ACS Appl. Mater. Interfaces*, 2015, **7**, 25970-25980.

64. M. Jannat and K.-L. Yang, *Langmuir*, 2018, **34**, 14226-14233.

65. Y. Zhu, Z. Huang, Q. Chen, Q. Wu, X. Huang, P.-K. So, L. Shao, Z. Yao, Y. Jia, Z. Li, W. Yu, Y. Yang, A. Jian, S. Sang, W. Zhang and X. Zhang, *Nat. Commun.*, 2019, **10**, 4049.

66. Y. Lv, Z. Lin, T. Tan and F. Svec, *Biotechnol. Bioeng.*, 2014, **111**, 50-58.

67. F. Liu, Y. Piao, J. S. Choi and T. S. Seo, *Biosens. Bioelectron.*, 2013, **50**, 387-392.

68. A. Gong, C.-T. Zhu, Y. Xu, F.-Q. Wang, F.-A. Wu and J. Wang, *Sci. Rep.*, 2017, **7**, 4309.

69. N. Singh, M. A. Ali, P. Rai, A. Sharma, B. D. Malhotra and R. John, *ACS Appl. Mater. Interfaces*, 2017, **9**, 33576-33588.

70. Z. Yin, W. Zhao, M. Tian, Q. Zhang, L. Guo and L. Yang, *Analyst*, 2014, **139**, 1973-1979.

71. D. Valikhani, J. M. Bolivar, M. Viefhues, D. N. McIlroy, E. X. Vrouwe and B. Nidetzky, *ACS Appl. Mater. Interfaces*, 2017, **9**, 34641-34649.

72. J. Liu, X. Jiang, R. Zhang, Y. Zhang, L. Wu, W. Lu, J. Li, Y. Li and H. Zhang, *Adv. Funct.*

View Article Online
DOI: 10.1039/C9RE00217K



*Mater.*, 2019, **29**, 1807326.

73. Y. Liu, W. Zhong, S. Meng, J. Kong, H. Lu, P. Yang, H. H. Girault and B. Liu, *Chem.: Eur. J.*, 2006, **12**, 6585-6591.

74. H. Bao, Q. Chen, L. Zhang and G. Chen, *Analyst*, 2011, **136**, 5190-5196.

75. Y. Bi, H. Zhou, H. Jia and P. Wei, *Process Biochem.*, 2017, **54**, 73-80.

76. G. H. Seong and R. M. Crooks, *J. Am. Chem. Soc.*, 2002, **124**, 13360-13361.

77. C. R. Boehm, P. S. Freemont and O. Ces, *Lab Chip*, 2013, **13**, 3426-3432.

78. S. Kundu, A. S. Bhangale, W. E. Wallace, K. M. Flynn, C. M. Guttman, R. A. Gross and K. L. Beers, *J. Am. Chem. Soc.*, 2011, **133**, 6006-6011.

79. J. Wang, X. Liu, X.-D. Wang, T. Dong, X.-Y. Zhao, D. Zhu, Y.-Y. Mei and G.-H. Wu, *Bioresour. Technol.*, 2016, **220**, 132-141.

80. G. H. Seong, J. Heo and R. M. Crooks, *Anal. Chem.*, 2003, **75**, 3161-3167.

81. L. C. Lasave, S. M. Borisov, J. Ehgartner and T. Mayr, *RSC Adv.*, 2015, **5**, 70808-70816.

82. D. N. Kim, Y. Lee and W.-G. Koh, *Sens. Actuators, B*, 2009, **137**, 305-312.

83. A. Kecskemeti and A. Gaspar, *Talanta*, 2017, **166**, 275-283.

84. T. Peschke, M. Skoupi, T. Burgahn, S. Gallus, I. Ahmed, K. S. Rabe and C. M. Niemeyer, *ACS Catal.*, 2017, **7**, 7866-7872.

85. R.-P. Liang, X.-N. Wang, C.-M. Liu, X.-Y. Meng and J.-D. Qiu, *J. Chromatogr. A*, 2013, **1315**, 28-35.

86. J. Sheng, L. Zhang, J. Lei and H. Ju, *Anal. Chim. Acta*, 2012, **709**, 41-46.

87. A. Karim, J. Bravo, D. Gorm, T. Conant and A. Datye, *Catal. Today*, 2005, **110**, 86-91.

88. J. M. Bolivar, J. Wiesbauer and B. Nidetzky, *Trends Biotechnol.*, 2011, **29**, 333-342.

89. D. J. Strub, K. Szymańska, Z. Hrydziuszko, J. Bryjak and A. B. Jarzębski, *React. Chem. Eng.*, 2019, **4**, 587-594.

90. M. Petro, F. Svec and J. M. Fréchet, *Biotechnol. Bioeng.*, 1996, **49**, 355-363.

91. T. R. Besanger, R. J. Hodgson, J. R. Green and J. D. Brennan, *Anal. Chim. Acta*, 2006, **564**, 106-115.

92. J. Qiao, L. Qi, X. Mu and Y. Chen, *Analyst*, 2011, **136**, 2077-2083.

93. A. S. de León, N. Vargas-Alfredo, A. Gallardo, A. Fernández-Mayoralas, A. Bastida, A. Muñoz-Bonilla and J. Rodríguez-Hernández, *ACS Appl. Mater. Interfaces*, 2017, **9**, 4184-4191.

94. K. Nakagawa and Y. Goto, *Chem. Eng. Process.*, 2015, **91**, 35-42.

95. J. P. Lafleur, S. Senkbeil, J. Novotny, G. Nys, N. Bøgelund, K. D. Rand, F. Foret and J. P. Kutter, *Lab Chip*, 2015, **15**, 2162-2172.

96. T. C. Logan, D. S. Clark, T. B. Stachowiak, F. Svec and J. M. Frechet, *Anal. Chem.*, 2007, **79**, 6592-6598.

View Article Online
DOI: 10.1039/C9RE00217K



97. D. S. Peterson, T. Rohr, F. Svec and J. M. Fréchet, *Anal. Chem.*, 2002, **74**, 4081-4088.

98. O. Yesil-Celiktas, S. Cumana and I. Smirnova, *Chem. Eng. J*, 2013, **234**, 166-172.

99. M. Alotaibi, J. Manayil, G. M. Greenway, S. J. Haswell, S. M. Kelly, A. F. Lee, W. Karen and G. Kyriakou, *React. Chem. Eng.*, 2017.

100. P. He, B. P. Burke, G. S. Clemente, N. Brown, N. Pamme and S. J. Archibald, *React. Chem. Eng.*, 2016, **1**, 361-365.

101. Y. Yi, Y. Chen, M. A. Brook and J. D. Brennan, *Chem. Mater.*, 2006, **18**, 5336-5342.

102. J. Ma, Z. Liang, X. Qiao, Q. Deng, D. Tao, L. Zhang and Y. Zhang, *Anal. Chem.*, 2008, **80**, 2949-2956.

103. P. Liang, H. Bao, J. Yang, L. Zhang and G. Chen, *Carbon*, 2016, **97**, 25-34.

104. D. Pirozzi, M. Abagnale, L. Minieri, P. Pernice and A. Aronne, *Chem. Eng. J*, 2016, **306**, 1010-1016.

105. D. N. Tran and K. J. Balkus Jr, *ACS Catal.*, 2011, **1**, 956-968.

106. J. Ma, L. Zhang, Z. Liang, W. Zhang and Y. Zhang, *J. Sep. Sci.*, 2007, **30**, 3050-3059.

107. J. Nelson and E. G. Griffin, *J. Am. Chem. Soc.*, 1916, **38**, 1109-1115.

108. T. Honda, H. Yamaguchi and M. Miyazaki, *Applied Bioengineering: Innovations and Future Directions*, 2017, **5**.

109. L. Cao, in *Carrier-bound Immobilized Enzymes*, Wiley-VCH Verlag GmbH & Co. KGaA, 2006, DOI: 10.1002/3527607668.ch2, pp. 53-168.

110. M. L. Shuler, F. Kargi and F. Kargi, *Bioprocess engineering: basic concepts*, Prentice Hall Upper Saddle River, NJ, 2002.

111. Z.-m. Tang and J.-w. Kang, *Anal. Chem.*, 2006, **78**, 2514-2520.

112. A. Srinivasan, H. Bach, D. H. Sherman and J. S. Dordick, *Biotechnol. Bioeng.*, 2004, **88**, 528-535.

113. G. Kulsharova, N. Dimov, M. P. Marques, N. Szita and F. Baganz, *New Biotechnol.*, 2017.

114. H. Mao, T. Yang and P. S. Cremer, *Anal. Chem.*, 2002, **74**, 379-385.

115. M. A. Holden, S.-Y. Jung and P. S. Cremer, *Anal. Chem.*, 2004, **76**, 1838-1843.

116. T. Vong, S. Schoffelen, S. F. van Dongen, T. A. van Beek, H. Zuilhof and J. C. van Hest, *Chem. Sci.*, 2011, **2**, 1278-1285.

117. Z.-Q. Wu, Z.-Q. Li, J.-Y. Li, J. Gu and X.-H. Xia, *Phys. Chem. Chem. Phys.*, 2016, **18**, 14460-14465.

118. K. Sakai-Kato, M. Kato and T. Toyo'oka, *Anal. Chem.*, 2003, **75**, 388-393.

119. H. Wu, Y. Tian, B. Liu, H. Lu, X. Wang, J. Zhai, H. Jin, P. Yang, Y. Xu and H. Wang, *J. Proteome Res.*, 2004, **3**, 1201-1209.

120. S.-i. Matsuura, R. Ishii, T. Itoh, S. Hamakawa, T. Tsunoda, T. Hanaoka and F. Mizukami, *Chem. Eng. J*, 2011, **167**, 744-749.

View Article Online
DOI: 10.1039/C9RE00217K



121. W.-G. Koh and M. Pishko, *Sens. Actuators, B*, 2005, **106**, 335-342.

122. A. A. Homaei, R. Sariri, F. Vianello and R. Stevanato, *Journal of Chemical Biology*, 2013, **6**, 185-205.

123. X. Ji, F. Ye, P. Lin and S. Zhao, *Talanta*, 2010, **82**, 1170-1174.

124. W. Min, W. Wang, J. Chen, A. Wang and Z. Hu, *Anal. Bioanal. Chem.*, 2012, **404**, 2397-2405.

125. J. J. Virgen-Ortíz, J. C. dos Santos, Á. Berenguer-Murcia, O. Barbosa, R. C. Rodrigues and R. Fernandez-Lafuente, *J. Mater. Chem. B*, 2017, **5**, 7461-7490.

126. S. Zhao, X. Ji, P. Lin and Y.-M. Liu, *Anal. Biochem.*, 2011, **411**, 88-93.

127. T.-F. Jiang, T.-T. Liang, Y.-H. Wang, W.-H. Zhang and Z.-H. Lv, *J. Pharm. Biomed. Anal.*, 2013, **84**, 36-40.

128. M. A. Camara, M. Tian, L. Guo and L. Yang, *J. Chromatogr. B*, 2015, **990**, 174-180.

129. Z. Tang, T. Wang and J. Kang, *Electrophoresis*, 2007, **28**, 2981-2987.

130. F. Wang, C. Guo, H.-Z. Liu and C.-Z. Liu, *J. Mol. Catal. B: Enzym.*, 2007, **48**, 1-7.

131. D. Kirstein, *Adv. Mol. Cell Biol.*, 1996, **15**, 247-256.

132. Q.-H. Shi, Y. Tian, X.-Y. Dong, S. Bai and Y. Sun, *Biochem. Eng. J.*, 2003, **16**, 317-322.

133. M. Miyazaki, J. Kaneno, R. Kohama, M. Uehara, K. Kanno, M. Fujii, H. Shimizu and H. Maeda, *Chem. Eng. J*, 2004, **101**, 277-284.

134. B. Brena, P. González-Pombo and F. Batista-Viera, *Immobilization of Enzymes and Cells: Third Edition*, 2013, 15-31.

135. P. C. Weber, D. Ohlendorf, J. Wendoloski and F. Salemme, *Science*, 1989, **243**, 85-88.

136. F. Rusmini, Z. Zhong and J. Feijen, *Biomacromolecules*, 2007, **8**, 1775-1789.

137. A. González‐Campo, B. Eker, H. J. Gardeniers, J. Huskens and P. Jonkheijm, *Small*, 2012, **8**, 3531-3537.

138. H. Schröder, L. Hoffmann, J. Müller, P. Alhorn, M. Fleger, A. Neyer and C. M. Niemeyer, *Small*, 2009, **5**, 1547-1552.

139. D. Liu, R. K. Perdue, L. Sun and R. M. Crooks, *Langmuir*, 2004, **20**, 5905-5910.

140. L. Lloret, G. Eibes, M. Moreira, G. Feijoo, J. Lema and M. Miyazaki, *Chem. Eng. J*, 2013, **223**, 497-506.

141. C. D. Blanchette, J. M. Knipe, J. K. Stolaroff, J. R. DeOtte, J. S. Oakdale, A. Maiti, J. M. Lenhardt, S. Sirajuddin, A. C. Rosenzweig and S. E. Baker, *Nat. Commun.*, 2016, **7**, 11900.

142. D. Simon, F. Obst, S. Haefner, T. Heroldt, M. Peiter, F. Simon, A. Richter, B. Voit and D. Appelhans, *React. Chem. Eng.*, 2019, **4**, 67-77.

143. S. Cumana, J. Simons, A. Liese, L. Hilterhaus and I. Smirnova, *J. Mol. Catal. B: Enzym.*, 2013, **85**, 220-228.

144. G. Ranieri, R. Mazzei, Z. Wu, K. Li and L. Giorno, *Molecules*, 2016, **21**, 345.

View Article Online
DOI: 10.1039/C9RE00217K



145. M. Bajić, I. Plazl, R. Stloukal and P. Žnidaršič-Plazl, *Process Biochem.*, 2017, **52**, 63-72.
146. H. Tan, S. Guo, N.-D. Dinh, R. Luo, L. Jin and C.-H. Chen, *Nat. Commun.*, 2017, **8**, 663.
147. H. Wang, Z. Zhao, Y. Liu, C. Shao, F. Bian and Y. Zhao, *Sci. Adv.*, 2018, **4**, eaat2816.
148. S. Fornera, P. Kuhn, D. Lombardi, A. D. Schlüter, P. S. Dittrich and P. Walde, *ChemPlusChem*, 2012, **77**, 98-101.
149. F. Costantini, R. Tiggelaar, S. Sennato, F. Mura, S. Schlautmann, F. Bordi, H. Gardeniers and C. Manetti, *Analyst*, 2013, **138**, 5019-5024.
150. T. Peschke, P. Bitterwolf, S. Gallus, Y. Hu, C. Oelschlaeger, N. Willenbacher, K. S. Rabe and C. M. Niemeyer, *Angew. Chem.*, 2018, **130**, 17274-17278.
151. R. J. Conrado, J. D. Varner and M. P. DeLisa, *Curr. Opin. Biotechnol*, 2008, **19**, 492-499.
152. Y.-H. P. Zhang, *Biotechnol. Adv.*, 2011, **29**, 715-725.
153. A. Küchler, M. Yoshimoto, S. Luginbühl, F. Mavelli and P. Walde, *Nat. Nanotechnol.*, 2016, **11**, 409-420.
154. T. Vong, S. Schoffelen, S. F. M. van Dongen, T. A. van Beek, H. Zuilhof and J. C. M. van Hest, *Chem. Sci.*, 2011, **2**, 1278-1285.
155. J. Grant, J. A. Modica, J. Roll, P. Perkovich and M. Mrksich, *Small*, 2018, **14**, 1800923.
156. G. Palazzo, G. Colafemmina, C. G. Iudice and A. Mallardi, *Sens. Actuators, B*, 2014, **202**, 217-223.
157. J. Heo, *Anal. Sci.*, 2014, **30**, 991-997.
158. S. Schoffelen and J. C. van Hest, *Current Opinion in Structural Biology*, 2013, **23**, 613-621.
159. J. Fu, M. Liu, Y. Liu, N. W. Woodbury and H. Yan, *J. Am. Chem. Soc.*, 2012, **134**, 5516-5519.
160. V. Hessel, C. Knobloch and H. Lowe, *Recent Pat. Chem. Eng.*, 2008, **1**, 1-16.
161. N. Kockmann, M. Gottsponer, B. Zimmermann and D. M. Roberge, *Chem.: Eur. J.*, 2008, **14**, 7470-7477.
162. N. Kockmann, M. Gottsponer and D. M. Roberge, *Chem. Eng. J.*, 2011, **167**, 718-726.
163. N. Kockmann and D. M. Roberge, *Chem. Eng. Process.*, 2011, **50**, 1017-1026.
164. P. Žnidaršič-Plazl, *Biotechnol. J.*, **0**, 1800580.
165. N. Miložič, M. Lubej, M. Lakner, P. Žnidaršič-Plazl and I. Plazl, *Chem. Eng. J*, 2017, **313**, 374-381.
166. F. Strniša, M. Bajić, P. Panjan, I. Plazl, A. M. Sesay and P. Žnidaršič-Plazl, *Chem. Eng. J*, 2018, **350**, 541-550.
167. A. Šalić, P. Faletar and B. Zelić, *Biochem. Eng. J.*, 2013, **77**, 88-96.
168. J.-i. Yoshida, *Flash chemistry: Fast organic synthesis in microsystems*, John Wiley & Sons, 2008.

View Article Online
DOI: 10.1039/C9RE00217K



169. S. J. Haswell and P. Watts, *Green Chem.*, 2003, **5**, 240-249.

170. S. G. Newman and K. F. Jensen, *Green Chem.*, 2013, **15**, 1456-1472.

171. C. Amador, A. Gavriilidis and P. Angeli, *Chem. Eng. J*, 2004, **101**, 379-390.

172. Z. Liu, J. Zhang, X. Chen and P. G. Wang, *ChemBioChem*, 2002, **3**, 348-355.

173. B. Orsat, B. Wirz and S. Bischof, *CHIMIA International Journal for Chemistry*, 1999, **53**, 579-584.

174. G. Gasparini, I. Archer, E. Jones and R. Ashe, *Org. Process Res. Dev.*, 2012, **16**, 1013-1016.

175. U. Novak, D. Lavric and P. Žnidaršiè-Plazl, *J. Flow Chem.*, 2016, **6**, 33-38.

176. S. Pithani, S. Karlsson, H. Emtenäs and C. T. Öberg, *Org. Process Res. Dev.*, 2019, DOI: 10.1021/acs.oprd.9b00240.

177. R. Das, H. Mishra, A. Srivastava and A. M. Kayastha, *Chem. Eng. J*, 2017, **328**, 215-227.

178. H.-L. Shuai, K.-J. Huang, Y.-X. Chen, L.-X. Fang and M.-P. Jia, *Biosens. Bioelectron.*, 2017, **89**, 989-997.

179. J. Sun, R. Yendluri, K. Liu, Y. Guo, Y. Lvov and X. Yan, *Phys. Chem. Chem. Phys.*, 2017, **19**, 562-567.

180. A. A. Kadam, J. Jang and D. S. Lee, *ACS Appl. Mater. Interfaces*, 2017, **9**, 15492-15501.

181. M. Z. Anwar, D. J. Kim, A. Kumar, S. K. Patel, S. Otari, P. Mardina, J.-H. Jeong, J.-H. Sohn, J. H. Kim and J. T. Park, *Sci. Rep.*, 2017, **7**, 15333.

182. X. Lian, Y. Fang, E. Joseph, Q. Wang, J. Li, S. Banerjee, C. Lollar, X. Wang and H.-C. Zhou, *Chem. Soc. Rev.*, 2017.

183. P. Li, J. A. Modica, A. J. Howarth, E. Vargas, P. Z. Moghadam, R. Q. Snurr, M. Mrksich, J. T. Hupp and O. K. Farha, *Chem*, 2016, **1**, 154-169.

184. Z. Li, H. Xia, S. Li, J. Pang, W. Zhu and Y. Jiang, *Nanoscale*, 2017, **9**, 15298-15302.

View Article Online
DOI: 10.1039/C9RE00217K

This review investigates the strategies of employing μ-IMERs for continuous biocatalysis by a top-down approach.